AMERICAN SOCIETY FOR MICROBIOLOGY | Journal of Virology®

TRANSFORMATION AND ONCOGENESIS

Polyomavirus Small T Antigen Induces Apoptosis in Mammalian Cells through the UNC5B Pathway in a PP2A-Dependent Manner

Sameer Ahmed Bhat,[a] Zarka Sarwar,[b] Syed Qaaifah Gillani,[b] Misbah Un Nisa,[b] Irfana Reshi,[a] Nusrat Nabi,[b] Shaozhen Xie,[c] Khalid M. Fazili,[a] Thomas M. Roberts,[c] Shaida Andrabi[b]

[a]Department of Biotechnology, University of Kashmir, Srinagar, India
[b]Department of Biochemistry, University of Kashmir, Srinagar, India
[c]Department of Cancer Biology, Dana Farber Cancer Institute, Harvard Medical School, Boston, Massachusetts, USA

ABSTRACT UNC5B is a dependence receptor that promotes survival in the presence of its ligand, netrin-1, while inducing cell death in its absence. The receptor has an important role in the development of the nervous and vascular systems. It is also involved in the normal turnover of intestinal epithelium. Netrin-1 and UNC5B are deregulated in multiple cancers, including colorectal, neuroblastoma, and breast tumors. However, the detailed mechanism of UNC5B function is not fully understood. We have utilized the murine polyomavirus small T antigen (PyST) as a tool to study UNC5B-mediated apoptosis. PyST is known to induce mitotic arrest followed by extensive cell death in mammalian cells. Our results show that the expression of PyST increases mRNA levels of UNC5B by approximately 3-fold in osteosarcoma cells (U2OS) and also stabilizes UNC5B at the posttranslational level. Furthermore, UNC5B is upregulated predominantly in those cells that undergo mitotic arrest upon PyST expression. Interestingly, although its expression was previously reported to be regulated by p53, our data show that the increase in UNC5B levels by PyST is p53 independent. The posttranslational stabilization of UNC5B by PyST is regulated by the interaction of PyST with PP2A. We also show that netrin-1 expression, which is known to inhibit UNC5B apoptotic activity, promotes survival of PyST-expressing cells. Our results thus suggest an important role of UNC5B in small-T antigen-induced mitotic catastrophe that also requires PP2A.

IMPORTANCE UNC5B, PP2A, and netrin-1 are deregulated in a variety of cancers. UNC5B and PP2A are regarded as tumor suppressors, as they promote apoptosis and are deleted or mutated in many cancers. In contrast, netrin-1 promotes survival by inhibiting dependence receptors, including UNC5B, and is upregulated in many cancers. Here, we show that UNC5B-mediated apoptosis can occur independently of p53 but in a PP2A-dependent manner. A substantial percentage of cancers arise due to p53 mutations and are insensitive to chemotherapeutic treatments that activate p53. Unexpectedly, treatment of cancers having functional p53 with many conventional drugs leads to the upregulation of netrin-1 through activated p53, which is counterintuitive. Therefore, understanding the p53-independent mechanisms of the netrin-UNC5B axis, such as those involving PP2A, assumes greater clinical significance. Anticancer strategies utilizing anti-netrin-1 antibody treatment are already in clinical trials.

KEYWORDS netrin 1, PP2A, polyomavirus, UNC5B, apoptosis, mitotic arrest, small T antigen

Citation Bhat SA, Sarwar Z, Gillani SQ, Un Nisa M, Reshi I, Nabi N, Xie S, Fazili KM, Roberts TM, Andrabi S. 2020. Polyomavirus small T antigen induces apoptosis in mammalian cells through the UNC5B pathway in a PP2A-dependent manner. J Virol 94:e02187-19. https://doi.org/10.1128/JVI.02187-19.

Editor Lawrence Banks, International Centre for Genetic Engineering and Biotechnology

Address correspondence to Shaida Andrabi, shaida.andrabi@uok.edu.in.

Received 10 January 2020
Accepted 2 May 2020
Accepted manuscript posted online 13 May 2020
Published 1 July 2020

Dependence receptors are a unique type of receptors that are capable of promoting either cell survival or cell death, depending upon ligand availability. Unlike the normal type of cell receptors that are activated solely upon ligand binding and initiate only one type of signaling inside the cells, these receptors are functional in both the bound and unbound states. Thus, they can transmit different types of signals which have opposite impacts on the host cell. UNC5 (A to D) proteins, p75 neurotrophin receptor ($p75^{NTR}$), and deleted in colon cancer (DCC) belong to this category of receptors. Mammals express four UNC5 receptors in the cell membrane: UNC5A, -B, -C, and -D (1–5), designated UNC5H1, -2, -3, and -4 in rodents. The UNC5B is a protein with an approximate size of 100 kDa that has three regions: extracellular, transmembrane, and intracellular. The extracellular region contains two immunoglobulin domains (IG) and two thrombospondin domains (TS) and is involved in ligand binding. The crystal structure of cytoplasmic portion of UNC5B has already been determined (6). It has three domains, namely, ZU5, UPA, and DD (death domain). The cytoplasmic region contains a caspase-3 cleavage site (7), and this region is involved in downstream signaling that involves DAPK1 activation. The extracellular domain binds multiple ligands, including netrin-1, netrin-3, and netrin-4 (4, 8–12). However, netrin-1 is the most studied among them. Upon netrin-1 binding to the extracellular domain, UNC5B initiates a survival pathway in the cells, while in the unbound state, it promotes apoptotic signaling (7). Death-associated protein kinase (DAPK) is constitutively associated with UNC5B. Binding of PP2A to DAPK1 leads to its dephosphorylation and resultant activation. The dephosphorylated DAPK in turn promotes activation of caspase-3 and initiates apoptosis. In contrast, binding of netrin-1 to UNC5B recruits the PP2A inhibitor CIP2A to the complex, thereby impeding the apoptotic pathway (13). The netrin-1/UNC5B pathway plays a very important role in regulating cell survival in mammalian cells.

Expression of UNC5B is known to be regulated by p53 (10), a well-known transcriptional factor that promotes apoptosis or cell cycle arrest at the G_1/S checkpoint. p53 binds to intron-1 of UNC5B and stimulates the transcription of UNC5B. p53 therefore exerts its apoptotic functions at least partly through the upregulation of UNC5B expression. On the other hand, netrin-1 binding to UNC5B promotes cell survival, partially by activating Akt signaling (14). Netrin-1 is involved in normal nervous system development and developmental angiogenesis (4, 15–17). Furthermore, netrin-1 and its receptors are associated with homeostatic maintenance of intestinal epithelium (18, 19). Both netrin-1 and UNC5 receptors are implicated in cancer development. Netrin-1 is upregulated and autocrinally synthesized in metastatic breast cancer, lung cancer, neuroblastoma, and pancreatic cancer (2, 18–21). On the other hand, expression of human UNC5A to -C is downregulated in many tumor types, including colorectal, breast, ovary, uterus, stomach, lung, and kidney cancers (22). Since netrin-UNC5B signaling is involved in multiple cellular pathways (23) and has diverse roles in normal physiology and in disease development, understanding the regulation and mechanism of this pathway has clinical significance.

Protein phosphatase 2A is an important cellular serine-threonine phosphatase that regulates numerous cellular functions in eukaryotic cells, including cell cycle regulation, DNA replication, transcription, translation, signal transduction, and apoptosis. It has three subunits: A, B, and C. The A subunit is the scaffolding subunit, whereas C is the catalytic subunit. Both subunits have two isoforms each: α and β. The regulatory B subunit in encoded by any one of many genes representing a very large number of isoforms, which make it complex. The B subunits are broadly categorized into four groups, B (B55), B′ (B56), B′′, and B′′′, and confer temporal and spatial specificity to PP2A complexes. PP2A A and B subunits are mutated in many types of cancers (24–27).

Multiple viral proteins of DNA tumor viruses are known to interact with and modulate PP2A activity by binding to one or more PP2A subunits. These notably include the middle T/small T antigen of the polyomavirus family of viruses (28, 29) and E4orf4 protein of adenoviruses (30). Exogenous expression of polyomavirus small T antigen (PyST) in mammalian cells is known to cause severe mitotic arrest followed by apoptosis in a PP2A-dependent manner (31, 32). Historically, it has been very difficult

to obtain stable cell lines expressing PyST because of its ability to induce mitotic arrest and apoptosis following acute expression of this protein. We previously circumvented that problem by making stable a cell line called pTREX-PyST-HA-FLAG that inducibly expresses small T antigen (32). However, the detailed mechanism of PyST-mediated apoptosis is not yet well understood. Here, we report that small T antigen expression in mammalian cells upregulates the expression of UNC5B, which promotes apoptosis in a p53-independent manner. We also observed that PyST expression induced apoptosis in various cancer cell lines, thus suggesting that this mechanism may have applications in treating different types of cancer. These studies are also important given the role of UNC5B in neural and vascular development and the turnover of intestinal epithelium on one hand and in tumorigenesis on the other hand.

RESULTS

Expression of PyST induced mitotic arrest and apoptosis in mammalian cells. Expression of PyST in mammalian cells is known to induce prolonged mitotic arrest followed by extensive cell death. The regulated U2OS cell line (pTREX-PyST-HA-FLAG) that stably expresses polyomavirus small T antigen was previously described (32). Expression of PyST in these cells is induced by the addition of doxycycline. Consistent with our previous findings (32), PyST expression caused overwhelming rounding up of U2OS cells and extensive cell death, as seen by microscopy and also detected by crystal violet staining (Fig. 1A and B). Increases in Bub1 expression and PARP1 cleavage were used to confirm mitotic arrest and apoptosis, respectively, in these cells (Fig. 1C). Recently, we have shown that PyST expression in U2OS cells changes the expression of commonly used loading controls such as tubulin, vinculin, and glyceraldehyde-3-phosphate dehydrogenase (GAPDH) (33); therefore, we have used Ponceau S staining as a loading control in experiments that involved PyST expression. We also confirmed mitotic arrest in PyST-expressing cells by immunofluorescence experiments, using an anti phospho-histone 3 serine 10 antibody. Our results showed an approximately 3.6-fold increase in mitotic index in PyST-expressing cells (Fig. 1D and E). This is an underestimate, because many mitotic cells, which are generally rounded up and hence less sticky, are lost during immunofluorescence experimental procedures. DAPI (4′,6-diamidino-2-phenylindole) staining also showed a substantial increase in the percentage of arrested mitotic cells, as evidenced by condensed chromosomal DNA in PyST-expressing cells (Fig. 1F). Mitotic arrest was clearly visible due to various abnormalities, including lack of chromosomal congression and predominantly prometaphase nuclear phenotype with almost no anaphase and telophase stages. Furthermore, fluorescence-activated cell sorting (FACS) analysis of PyST-expressing cells showed increases in the G_2/M and sub-G_1 peaks, indicating mitotic arrest and cell death, respectively (Fig. 1G and H). We also observed that PyST expression induced mitotic arrest and apoptosis in various cancer cell lines, though their sensitivities to PyST expression varied as they took different durations to show the rounded up mitotic phenotypes as indicated (Fig. 1I). We, however, noted that the rat glioma C6 cell line had a very modest mitotic arrest phenotype even after 9 days of doxycycline addition, indicating that they are resistant to PyST-induced mitotic arrest. Western blotting for mitotic markers such as Bub1 confirmed that these cell lines, except for C6, were indeed arrested in mitosis (Fig. 2E and F), which was consistent with the observed phenotypes as shown in Fig. 1I. These results are significant, as they suggest that many cancer cell lines are sensitive to PyST expression-induced mitotic arrest and apoptosis.

UNC5B is upregulated in PyST-expressing cells following mitotic arrest. Though it is well established that the small T antigen's ability to induce cell death is dependent upon its interaction with protein phosphatase 2A (PP2A) (31), the detailed mechanism by which PyST expression causes cell death is not well understood. To get deeper insights into these details, whole-genome microarray analysis was performed on total cellular RNA obtained from this inducible PyST-expressing cell line by using Affymetrix human genome U133 Plus 2.0 (HG-U133_Plus_2) chips. RNA was isolated simultaneously from these cells in triplicates at approximately 20 h of doxycycline addition when

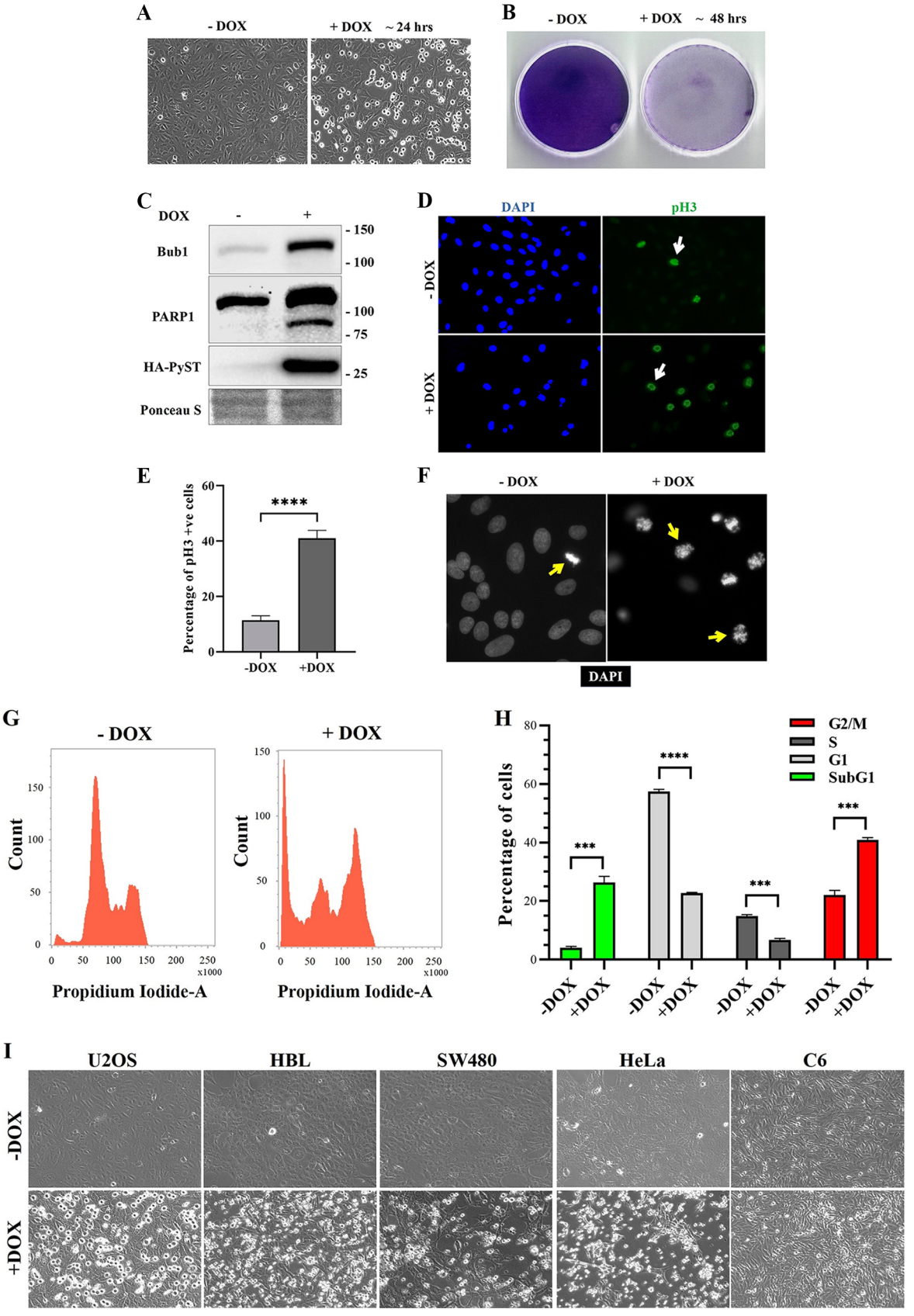

FIG 1 Expression of PyST induces mitotic arrest and apoptosis in mammalian cells. (A) Doxycycline (10 μg/ml) was added for approximately 24 h to PyST-U2OS cells (+DOX), and cells were visualized by microscopy (×10 magnification). (B) Doxycycline (10 μg/ml) was added for

(Continued on next page)

the mitotic phenotype, as indicated by extensive cell rounding, was clearly visible. The data revealed more than 900 genes that had 1.5-fold or greater levels of change in RNA expression compared to that in the control uninduced cells (*P* values, 0.000081 to 0.049936). We considered $\log_2$ fold change for subsequent data analyses, which yielded approximately 100 genes that were most notably affected by PyST expression (*P* value, 0.000081 to 0.009525), as shown in the heat map (Fig. 2A). The data obtained from these experiments were quite consistent with the phenotype, as most of the genes whose expression was affected in this cell line are involved in cell cycle regulation, particularly mitosis and apoptosis. Since PyST expression leads to cell death, one gene that particularly caught our attention was UNC5B because of its known role in apoptosis. Microarray data showed that expression of UNC5B was elevated by approximately 2.7-fold (*P* value, 0.003063) in small-T antigen-expressing cells (plus doxycycline [+DOX]) compared to that in the uninduced controls (minus doxycycline [−DOX]), as shown in the heat map (Fig. 2A). In contrast, expression of other dependence receptors of this family (UNCA, -C, and -D) was not affected. These data are available online at NCBI/GEO (accession number GSE149525). To get an idea about which cellular pathways were affected by PyST expression, we performed a gene set enrichment analysis (GSEA) using microarray data. Interestingly, GSEA showed upregulated expression of numerous genes associated with apoptosis. Among these genes, UNC5B was the most significantly affected candidate in PyST-expressing (+DOX) cells (Fig. 2B) (data not shown).

Next, we wanted to confirm the microarray data by real-time quantitative PCR (RT-qPCR) and Western blotting. RT-qPCR performed with mRNA obtained at approximately 30 h postdoxycycline addition revealed that UNC5B mRNA levels were indeed increased by approximately 3-fold in PyST-expressing cells (Fig. 2C). Using Western blotting, a visible time-dependent increase in UNC5B levels was observed starting from 16 h of doxycycline addition, which was proportionate to the increase in PyST expression (Fig. 2D and E). Though there was no further significant increase in PyST expression after 24 h of doxycycline addition, UNC5B levels were maximally increased at the 40-h time point. Next, we checked if PyST increased UNC5B expression in some other cell lines as well. Interestingly, we found that besides U2OS, PyST also upregulated UNC5B protein levels in various cell lines, namely, HBL (breast cancer) and SW480 (colon cancer), while HeLa (cervical cancer) and C6 (rat glioma) cells had a modest increase (Fig. 2F and G). These results were mostly in accordance with the observed mitotic phenotype of these cell lines as shown in Fig. 1I. For HeLa cells, though the UNC5B increase was not pronounced at this time point (48 h), they did show the mitotic phenotype. It is possible that the increase in UNC5B levels occurred at a later time point.

We were curious to know whether the increase in UNC5B expression occurs specifically in response to PyST expression or can also occur as a result of general toxicity in

FIG 1 Legend (Continued)
approximately 48 h to PyST-U2OS (+DOX) cells, and adherent cells were fixed and stained with crystal violet solution. (C) Doxycycline was added for 32 h to PyST-U2OS cells (+DOX), and cell lysates were blotted for Bub1 and PARP1 expressions using appropriate antibodies. Ponceau S was used as loading control. (D) Immunofluorescence was measured using anti-phospho-histone 3 serine 10 (pH3 S10) antibody in control (−DOX) and PyST-expressing (+DOX; 24 h) cells. DAPI was used to stain the nuclei. Pictures were taken at ×20 magnification. (E) pH3 immunofluorescence was analyzed in control cells ($n = 337$) and PyST-expressing cells ($n = 380$), and percentages of pH3-positive cells were compared using *t* test in GraphPad Prism. Graph indicates comparison of percentages of pH3-positive cells in control (−DOX) and PyST-expressing U2OS cells (+DOX). Values indicate means ± standard errors of the means (SEMs); $n = 7$ for −DOX and $n = 14$ for +DOX (where *n* represents the number of immunofluorescence fields of image) used for counting percentages of pH3-positive cells. ****, $P < 0.0001$ (two-tailed unpaired Student's *t* test). (F) Doxycycline was added to PyST-U2OS cells for 30 h, and cells were fixed and stained with DAPI to visualize DNA. Normal mitosis can be seen in control cells. However, PyST expression arrests the cells predominantly in prometaphase as shown by arrows (×20 magnification). (G) Doxycycline was added for approximately 30 h to PyST-U2OS cells, and cells were analyzed for cell cycle analysis by flow cytometry. (H) Graph representing comparison of percentages of cells in different phases of cell cycle (as indicated) in control (−DOX) and PyST-expressing U2OS cells (+DOX). Values indicate means ± SEMS; $n = 3$ replicates. ****, $P < 0.0001$, ***, $P = 0.0001$ to 0.001 (two-tailed unpaired Student's *t* test). (I) Different stable cell lines expressing PyST showed mitotic arrest and apoptotic phenotype after doxycycline addition. Cells were plated at equal densities and treated with doxycycline (+DOX) until the mitotic phenotype (rounding up) was visible: U2OS, 24 h; HBL, 7 days; SW480, 3 days; HeLa, 48 h; and C6, 9 days. Pictures were taken at ×10 magnification.

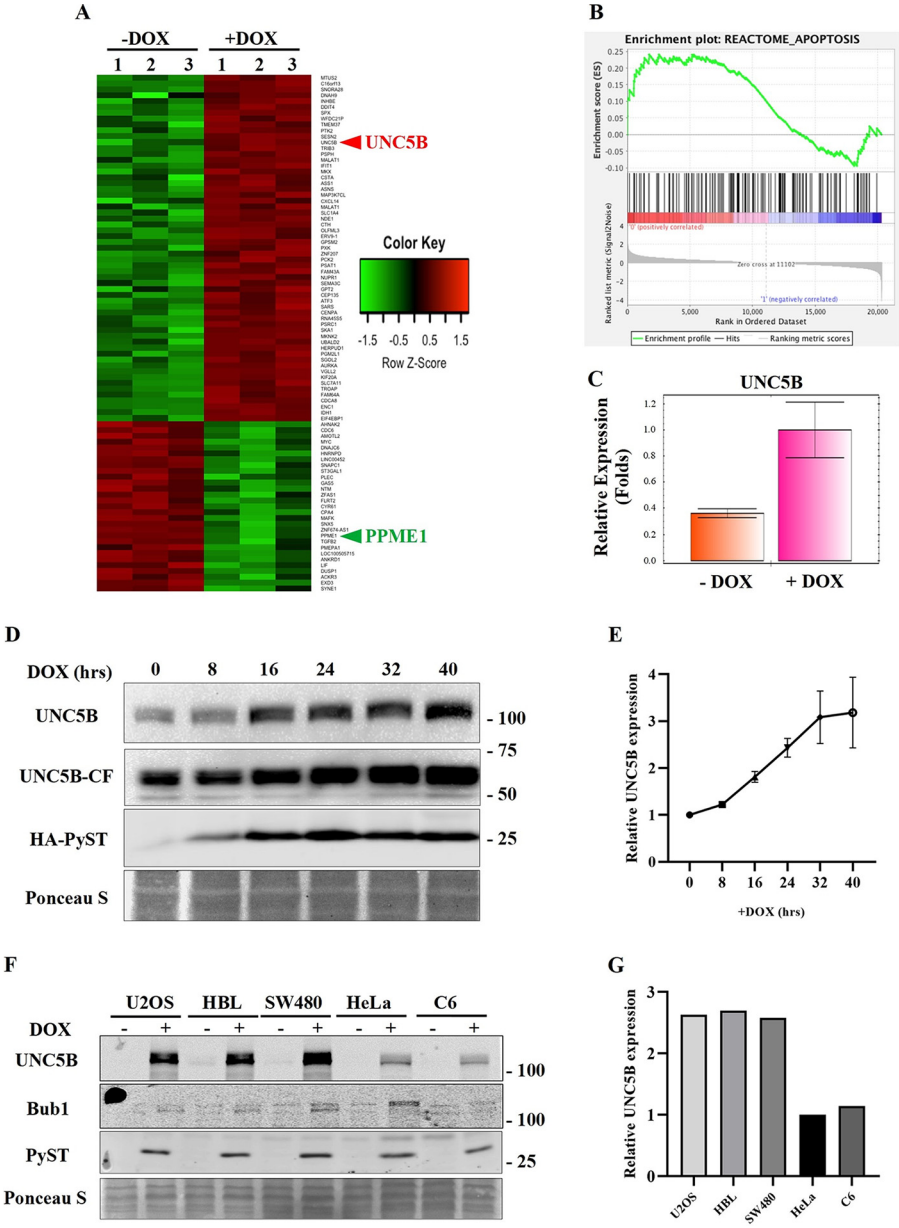

FIG 2 UNC5B is upregulated in PyST expressing cells. (A) Microarray analysis of whole human genome using total cellular RNA obtained from PyST-expressing U2OS stable cell lines was carried out in triplicates, in the absence and presence of PyST expression (−DOX and +DOX, respectively). Change in expression of genes that were affected by $\log_2$ fold or more is shown in the heat map. UNC5B location on the heat map is highlighted and indicated by an arrow. (B) Gene set enrichment analysis (GSEA) showed that the expression of genes in the apoptosis pathway was enriched in DOX-treated cells (False discovery rate [q] $<$ 0.5). (C) Doxycycline was added for approximately 30 h to PyST-U2OS cells, and UNC5B mRNA expression was analyzed by RT-qPCR. Experiments were performed in duplicates, and the gene expression normalized to actin expression ($\Delta\Delta C_q$) was calculated by using Bio-Rad CFX Manager. (D) Doxycycline was added for the indicated time periods in the same cell line, and cell lysates were blotted for UNC5B expression using an anti-UNC5B antibody. (E) Graph representing relative UNC5B expression at different time periods of doxycycline addition compared with control (0 h of DOX addition) UNC5B expression, which was arbitrarily taken as 1. Values indicate means ± SEMs; $n = 3$ for 16 h, $n = 4$ for 24 and 32 h, and $n = 2$ for 40 h of DOX addition, where n represents the number of biological replicates. (F) Western blotting was used to confirm UNC5B upregulation, mitotic arrest (by Bub1 expression), and PyST expression upon doxycycline addition (at corresponding time points as mentioned in the legend for Fig. 1I) in different cell lines as indicated using appropriate antibodies as shown. (G) Graph representing relative UNC5B expression in various PyST-expressing cell lines normalized to PyST levels. The lowest UNC5B protein level in C6 cells was arbitrarily taken as 1, and UNC5B levels in other cell lines were calculated as fold changes with respect to the level in C6 cells. (H) U2OS cells were given different treatments overnight (16 h), and cell lysates were blotted for UNC5B expression. Strv, starvation; Etop, etoposide, 50 μM; Hu, hydroxyurea, 5 mM; Noc, nocodazole, 100 ng/ml; Pac, paclitaxel, 500 nM. Dimethyl sulfoxide (DMSO) was used as vehicle control (Con). (I) Graphical representation of the fold expression as depicted in panel H. Values indicate means ± SEMs; $n = 2$ for Strv and Pac, $n = 4$ for Etop and Hu, and $n = 3$ for Noc, where n represents the number of biological replicates. (J) UNC5B expression was detected by immunofluorescence microscopy at ×63 magnification (DOX, 30 h). DAPI was used to stain the nuclei, and anti-tubulin antibody was used to stain the cytoskeleton. In control (−DOX) cells, arrows indicate cells in metaphase (top) and anaphase (bottom). In PyST-expressing cells (+DOX), yellow arrow indicates cells in interphase, while white arrow shows cells in mitosis. (K) One cell was chosen from the control (−DOX) and PyST-expressing cells (+DOX) from the experiments as shown in panel J and magnified to highlight the expression of UNC5B along the plasma membrane.

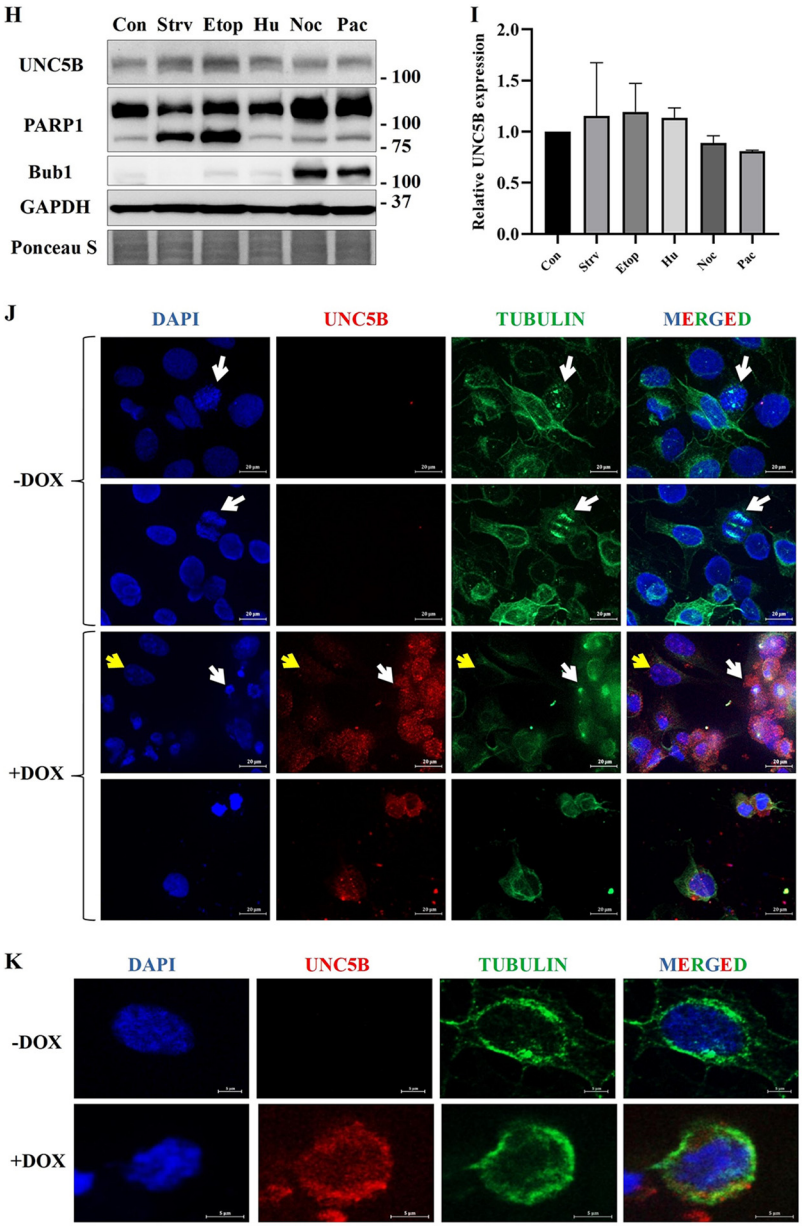

FIG 2 (Continued)

response to various DNA-damaging and/or apoptosis-inducing stimuli. To test that, U2OS cells were subjected to various cytotoxic treatments. Results showed that general cytotoxicity does not increase UNC5B levels (Fig. 2H and I), though these treatments did provoke an apoptotic response, as was revealed by PARP1 cleavage. Even drugs such as nocodazole and paclitaxel (34), which are well known to induce mitotic arrest, did not increase UNC5B levels until 24 h of treatment. This suggested that activation of UNC5B is specific to PyST-induced mitotic arrest/apoptosis and may need some additional stimuli or cellular interactors (i.e., protein-protein interactions) that these drugs may not be able to provide or stimulate.

Immunofluorescence microscopy results also showed that PyST expression substantially increased UNC5B levels, particularly in those cells that underwent mitotic arrest as identified by cell rounding and chromatin condensation using DAPI staining (Fig. 2J). UNC5B expression was clearly seen in cells that were induced for PyST expression, indicating its higher expression in the presence of doxycycline (+DOX), while no

staining was seen in control cells (−DOX). Interestingly, UNC5B expression was much more prominent in PyST-expressing cells (+DOX) that were in mitotic phase (white arrows) than in those in the interphase stage (yellow arrows). This staining of UNC5B along the cell membrane boundary is seen more clearly in Fig. 2K. In contrast, control cells (−DOX) had no visible UNC5B staining either in interphase or in mitosis (Fig. 2K, as indicated by arrows showing metaphase [top] and anaphase [bottom]). Mitotic cells are indicated by DAPI (chromosomal congression) and tubulin (centrosome) staining in control cells (−DOX). Putting these data together, it can be inferred that UNC5B expression is stimulated in response to mitotic arrest-induced apoptosis in PyST-expressing cells.

The increase in UNC5B protein levels by PyST is p53 independent. UNC5B expression at the transcriptional level was previously shown to be regulated by p53 (10, 35). Since both UNC5B and p53 have an important role in apoptosis, we wanted to test whether UNC5B expression in PyST-expressing cells is also regulated by p53. Though real-time quantitative PCR data showed an increase in p53 levels at the mRNA level in cells expressing PyST (Fig. 3A), Western blotting results, however, showed that PyST expression decreases p53 expression at a time period where UNC5B levels are elevated by PyST (Fig. 3B and C), thus indicating that UNC5B protein levels may not be regulated by p53 in PyST-expressing cells. To further support our data, we also inhibited endogenous p53 activity by making a stable cell line expressing dominant negative p53 in PyST-U2OS cells. Expression of dominant negative p53 in U2OS cells was confirmed by Western blotting (Fig. 3D). We found that overexpression of PyST induced mitotic arrest as well as apoptosis in both control (PyST) and dominant negative p53-expressing cells (DNp53) to an almost equal extent, as was evident by cell morphologies at both 24 and 48 h (Fig. 3E). In similar experiments, PyST (control [Con]) and DNp53-PyST (DNp53) cells were subjected to crystal violet staining at 48 h after doxycycline addition (Fig. 3F). These results were also consistent with the above phenotype. Further support came from PARP1 blotting results, which showed comparable expression/cleavage levels between control and DNp53 cells expressing PyST upon doxycycline addition (Fig. 3G). All of these results were consistent with our previous findings that PyST-induced apoptosis is independent of p53 (32). Consistent with these data, UNC5B protein levels were still elevated by PyST expression even in the presence of DNp53 (Fig. 3H and I). This suggested that the increase in UNC5B levels by PyST is regulated by a p53-independent mechanism. To confirm that DNp53 cells truly had a defective p53 response, both U2OS control and U2OS-DNp53 cell lines were treated for 2 days with different drugs that typically provoke a p53 response: aphidicolin (10 μM), hydroxyurea (2 mM), and etoposide (2 μM). Prolonged exposure to these drugs is known to induce cell death in various cell lines (36, 37). Our results showed that while control U2OS cells were arrested and died when treated with these drugs, the dominant negative cells were substantially resistant to cell cycle arrest and apoptosis, thus confirming that these cells had a defective p53 response (Fig. 3J). We obtained similar results by crystal violet staining, confirming that DNp53-overexpressing cells had a truly defective p53 pathway (Fig. 3K).

PyST stabilizes UNC5B expression in a PP2A-dependent manner. The UNC5B pathway was previously extensively studied in HEK 293T cells also, where it has been shown to induce apoptosis (7, 13, 14, 22, 35, 38). An additional reason for using 293T cells was that, compared to that of most other cell lines, they have very high transfection efficiency and also express exogenously transfected genes at high levels. To check whether PyST expression has any effect on UNC5B protein levels in HEK 293T cells also, hemagglutinin (HA)-UNC5B and PyST constructs were cotransfected in these cells. Interestingly, it was seen that exogenous HA-UNC5B protein amounts were elevated in these transfected cells, with UNC5B levels proportional to the amounts of PyST transfected (Fig. 4A). pCDNA-topo-UNC5B used for transient transfections has a constitutive viral promoter (cytomegalovirus [CMV]) that does not contain the endogenous UNC5B gene promoter elements. With numerous other experiments also, we have observed

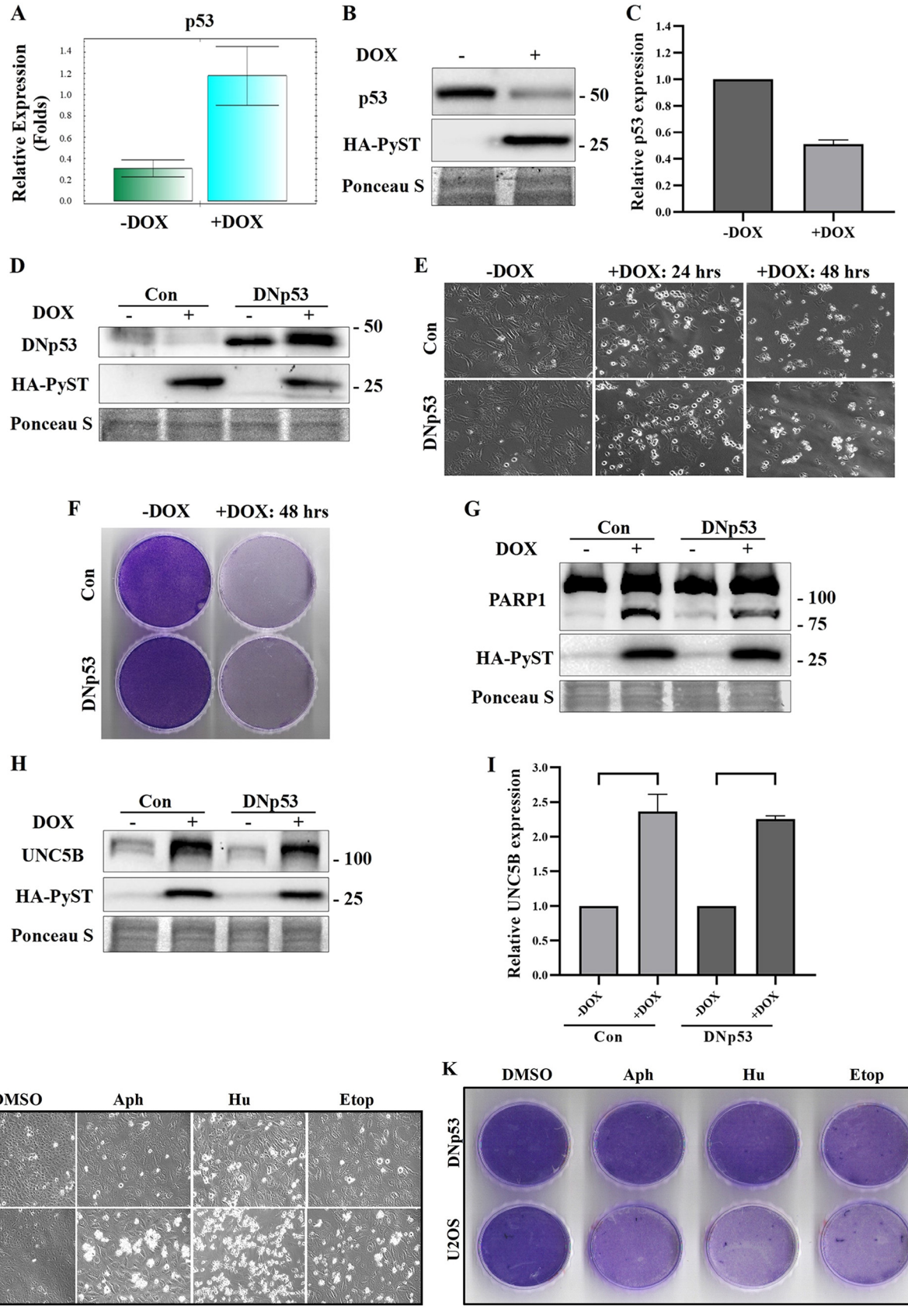

FIG 3 PyST-induced mitotic arrest and increase in UNC5B amounts are p53 independent. (A) Doxycycline was added for approximately 30 h to PyST-expressing U2OS cells, and p53 expression was analyzed by RT-qPCR. Data were normalized to actin expression, and gene expression was

(Continued on next page)

that PyST does not increase the basal promoter activity of many expression vectors during transient transfections (data not shown). These results suggested that, in addition to increasing the endogenous expression of UNC5B at the mRNA level, PyST might be involved in increasing its stability at the posttranslational level as well. To confirm this, cycloheximide (CHX) assays were performed with 293T cells for different time intervals. Results showed that PyST expression indeed increased the stability of UNC5B protein levels (Fig. 4B and C).

PyST is well known to bind heat shock proteins (HSPs) and PP2A via its N-terminal J domain and C-terminal regions, respectively (Fig. 4D) (39). Most of the critical PyST functions in mammalian cells, including the induction of mitotic arrest/apoptosis, are dependent upon its ability to bind PP2A (31). To check the role of these PyST domains in UNC5B upregulation, we used PyST mutants, which are unable to bind PP2A (PP2A−) or heat shock proteins (HSP−). BC1075 (PP2A−) is a PyST mutant in which the cysteine 142 has been mutated to a tyrosine residue and consequently does not bind PP2A (31, 40, 41), while the PyST D44N construct (HSP−) has a J domain in which the HPDKGG motif has been mutated at residue 44. The HPDKGG motif is conserved in the J domain of all T antigens of the polyomavirus family, and mutation in this region affects their ability to bind heat shock proteins (42–45). Our results showed that coexpression of the HSP− mutant of PyST (D44N) increased UNC5B protein levels similarly as wild-type PyST. In contrast, the PP2A− mutant (BC1075) was defective in this role (Fig. 4E and F). Hence, increase in UNC5B protein levels is dependent upon the ability of PyST to bind PP2A, which is consistent with the dependence of PyST on PP2A binding to induce apoptosis.

Unbound UNC5B was previously shown to promote cell death by recruiting PP2A complex via its C-terminal domain on the cytoplasmic side (13). It was intriguing to find out which specific subunits of PP2A are involved in this mechanism of UNC5B regulation. We transiently expressed many PP2A subunit isoforms along with UNC5B to check their impact on UNC5B protein levels. Interestingly, our results showed that overexpression of Aβ and Cα subunits increased UNC5B protein levels (Fig. 4G). Also, many B subunit isoforms, particularly B55α and B56ε, were individually capable of increasing UNC5B protein levels (Fig. 4H). The relative changes in UNC5B amounts in the presence of different subunits of PP2A as shown in Fig. 4G and H are shown graphically in Fig. 4I. We believe that these specific subunits of PP2A have an important role in promoting stabilization of UNC5B and hence promoting apoptosis through this signaling pathway. Our results are consistent with the earlier reports in which UNC5B apoptotic activity was shown to involve the Aβ subunit (13). The identity of other PP2A subunits that affect UNC5B activity has, however, not been reported. It was also quite interesting to note that the mRNA expression of protein phosphatase methylesterase 1 (PPME1), an endogenous cellular PP2A inhibitor (46–50), was also downregulated by approximately 2-fold in PyST-expressing cells (+DOX) (Fig. 4J and 2A, heat map). That it was among the top 20 downregulated genes in the microarray analysis data indicates its importance in regulating PP2A (and possibly UNC5B)-mediated signaling in PyST-expressing cells.

FIG 3 Legend (Continued)

calculated by using Bio-Rad CFX Manager. (B) Cell lysates were blotted for p53 expression using anti-p53 antibody (DOX, 32 h). (C) Graph representing relative p53 expression in PyST-expressing U2OS cells (+DOX) compared with that in control cells (−DOX), where the expression was arbitrarily taken as 1. Values indicate means ± SEMS; $n = 3$ biological replicates. (D) PyST-expressing (Con) and DNp53-PyST (DNp53) cell lysates were subjected to Western blotting to detect the expression of dominant negative p53, using antibodies against p53. Expression of PyST after doxycycline addition was confirmed using an anti-HA antibody. Ponceau S staining was used as a loading control. (E) Doxycycline was added for approximately 24 h and 48 h in PyST (Con) and dominant negative expressing PyST-U2OS cells (DNp53), and cell morphologies (rounding up) were observed. Pictures were taken at ×10 magnification. (F) PyST-expressing (Con) and DNp53-PyST (DNp53) cells were treated with doxycycline for 48 h and stained with crystal violet to compare cell densities. Cell lysates were blotted for PARP1 expression/cleavage (G) and for UNC5B expression (H) (+DOX, 30 h). Ponceau S staining was used as a loading control. (I) Graph representing relative UNC5B expression (as in panel H) in control (PyST-U2OS) and DNp53-expressing cells. UNC5B levels under the −DOX conditions were arbitrarily taken as 1. Values indicate means ± SEMs; $n = 2$ biological replicates. (J) Control (bottom) and DNp53-expressing U2OS cells (top) were subjected to different treatments that elicit the DNA damage response and block DNA synthesis. Aphidicolin (Aph), 10 μM; hydroxyurea (Hu), 2 mM; etoposide (Etop), 2 μM. DMSO was used as vehicle control. Time, 24 h of drug treatment; ×10 magnification. (K) Control U2OS and DNp53-expressing cells were subjected to treatment as in panel H, fixed, and stained with crystal violet to compare cell densities. Experiments were repeated 2 to 3 times.

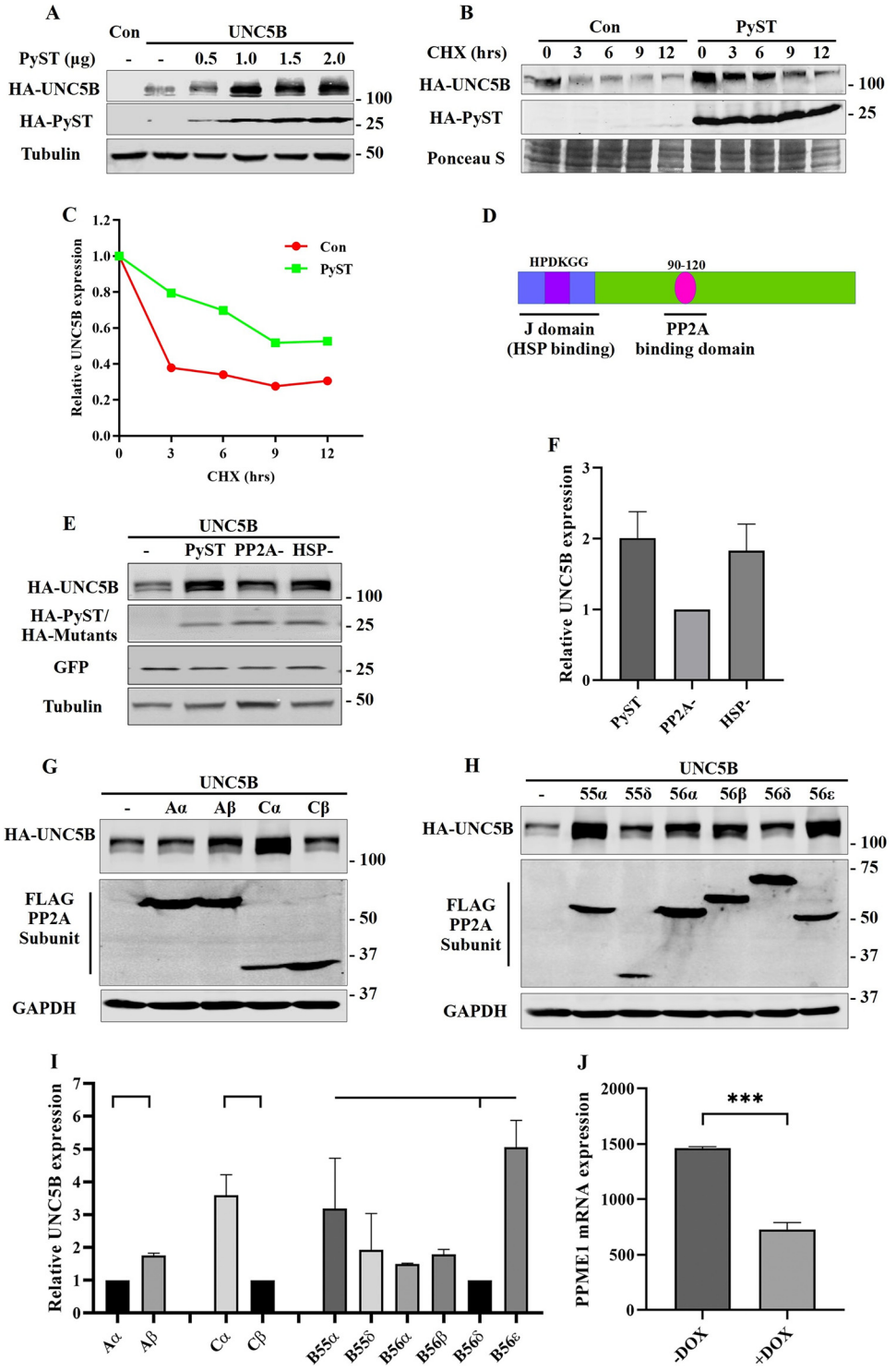

FIG 4 PyST promotes posttranslational stabilization of UNC5B. (A) pCDNA-UNC5B-HA and increasing amounts of pCDNA-PyST-HA (as indicated) were transiently transfected in HEK 293T cells, and cell lysates were blotted for UNC5B and PyST expressions using and anti-HA antibody. (B and C) UNC5B (1 μg) was transfected in HEK 293T cells with or without PyST (1 μg). After 2 days, cells were treated with 25 μg/ml CHX for different time points as indicated. Cell lysates were then blotted for UNC5B expression using an anti-HA antibody. After normalizing initial protein levels, graphs were drawn for UNC5B levels alone or in the presence of PyST. (D) Diagram depicting positions on PyST protein where heat shock proteins (HSPs) and PP2A bind. (E) HEK 293T cells were transiently transfected with constructs expressing UNC5B-HA (1.0 μg), Pinco-GFP (0.5 μg), and wild-type PyST or its mutants BC1075 (PP2A−) or D44N (HSP−) (1.0 μg each). Cell lysates were blotted for expression of UNC5B and PyST and its mutants using an anti-HA antibody. Pinco-GFP construct was used as a transfection control and was blotted with an anti-GFP antibody. Tubulin was also used as a loading control. (F) Graph representing relative UNC5B protein

(Continued on next page)

Exogenous UNC5B expression slows the growth of U2OS cells and induces apoptosis. As shown in previous results, UNC5B levels were increased in PyST expression in a U2OS background. Overexpression of UNC5B is known to promote cell death in the absence of netrin-1. To find out whether expression of UNC5B by itself (in the absence of PyST expression) could also induce apoptosis in U2OS cells, we made a stable U2OS cell line with inducible expression of UNC5B. Expression of UNC5B was induced by doxycycline addition (Fig. 5A), and cells were visualized by microscopy or crystal violet staining (Fig. 5B and C). There was a clear decrease in the density of cells upon UNC5B expression. Quantification via crystal violet staining of cells grown for 3 days in doxycycline showed that there was an approximately 25% decrease in cell density (Fig. 5D). We wanted to independently confirm whether the decrease in cell density occurred as a consequence of apoptosis in these cells. Results showed that at 48 h of doxycycline addition, UNC5B expression promoted an increase in expression as well as in cleavage of PARP1 (Fig. 5E and F). Thus, UNC5B expression alone slows growth and induces apoptosis in U2OS cells. The cell death induced on its own by UNC5B overexpression is, however, clearly less than that induced by PyST, thus indicating that cell death by UNC5B might need some additional stimuli.

Inhibition of UNC5B by netrin-1 promotes cell survival. Binding of netrin-1 to the UNC5B receptor is known to inhibit cell death (7, 12, 14, 15). We wondered whether the weak apoptotic phenotype in UNC5B-overexpressing cells in the previous experiment (Fig. 5) was because of the endogenous expression of netrin-1 by U2OS cells, which would bind to UNC5B extracellularly and inhibit apoptotic signaling. Western blotting did not show any endogenous netrin-1 protein expression in U2OS cells in the absence or presence of PyST expression either in the cell lysates or in the culture medium (Fig. 6A). Together with results in Fig. 5, these data suggested that the modest apoptotic phenotype in U2OS cells in response to UNC5B expression may not be because of extracellular netrin-1 availability. Rather, it could be due to the lack of an additional signal that may be needed to provoke UNC5B-mediated apoptotic signaling. In order to determine the significance of increased UNC5B expression in the PyST background, a U2OS cell line with constitutive expression of netrin-1 was constructed in PyST-U2OS cells (Fig. 6B). Even though the induction of PyST expression decreased the netrin-1 levels appreciably, significant levels of netrin-1 were maintained which would potentially bind the UNC5B receptors. Our results showed that netrin-1 expression decreased PARP1 cleavage induced by PyST (Fig. 6C and D), thus indicating a decrease in apoptosis in the presence of netrin-1. We also observed a decrease in Bub1 expression in netrin-1-expressing cells, which indicates a decrease in the percentage of cells arrested in mitotic phase (Fig. 6E and F). When control and netrin-1-expressing PyST-U2OS cells were grown in the presence of doxycycline for several days, substantial number of PyST-resistant colonies were observed in netrin-1-expressing cells, as visualized by crystal violet staining of adherent cells (Fig. 6G). These results suggested that netrin-1 promotes survival in PyST-expressing cells and that UNC5B overexpression and stabilization plays an important role in PyST-induced apoptosis.

DISCUSSION

In this study, we found that expression of PyST increases the expression of UNC5B in several cell lines. Apart from increasing the mRNA levels, we found that PyST

FIG 4 Legend (Continued)
levels in cells transfected with PyST-, PP2A-, and HSP-expressing constructs. Normalization was to the protein levels of PyST and its mutants. Protein level of UNC5B in the lane transfected with PP2A− construct (with the lowest expression) was arbitrarily taken as 1. Values indicate means ± SEMs; $n = 3$ biological replicates. (G and H) HEK 293T cells were transfected with UNC5B-HA and different FLAG-PP2A subunit constructs as indicated (1.0 μg each). Cell lysates were blotted for exogenously expressing HA-UNC5B and FLAG-PP2A subunits using anti-HA and anti-FLAG antibodies, respectively. (I) Graph representing relative UNC5B expression in cells transfected with PP2A subunit isoforms. Normalization was to the protein levels of the isoforms. In each case, protein levels of the isoform with the lowest expression were arbitrarily taken as 1. Values indicate means ± SEMs; $n = 2$ biological replicates. (J) Graph representing PPME1 mRNA expression detected by microarray analysis in PyST-U2OS cells under the −DOX and +DOX conditions. Values indicate means ± SEMs; $n = 3$ replicates. ***, $P = 0.0001$ to 0.001 (two-tailed unpaired Student's t test).

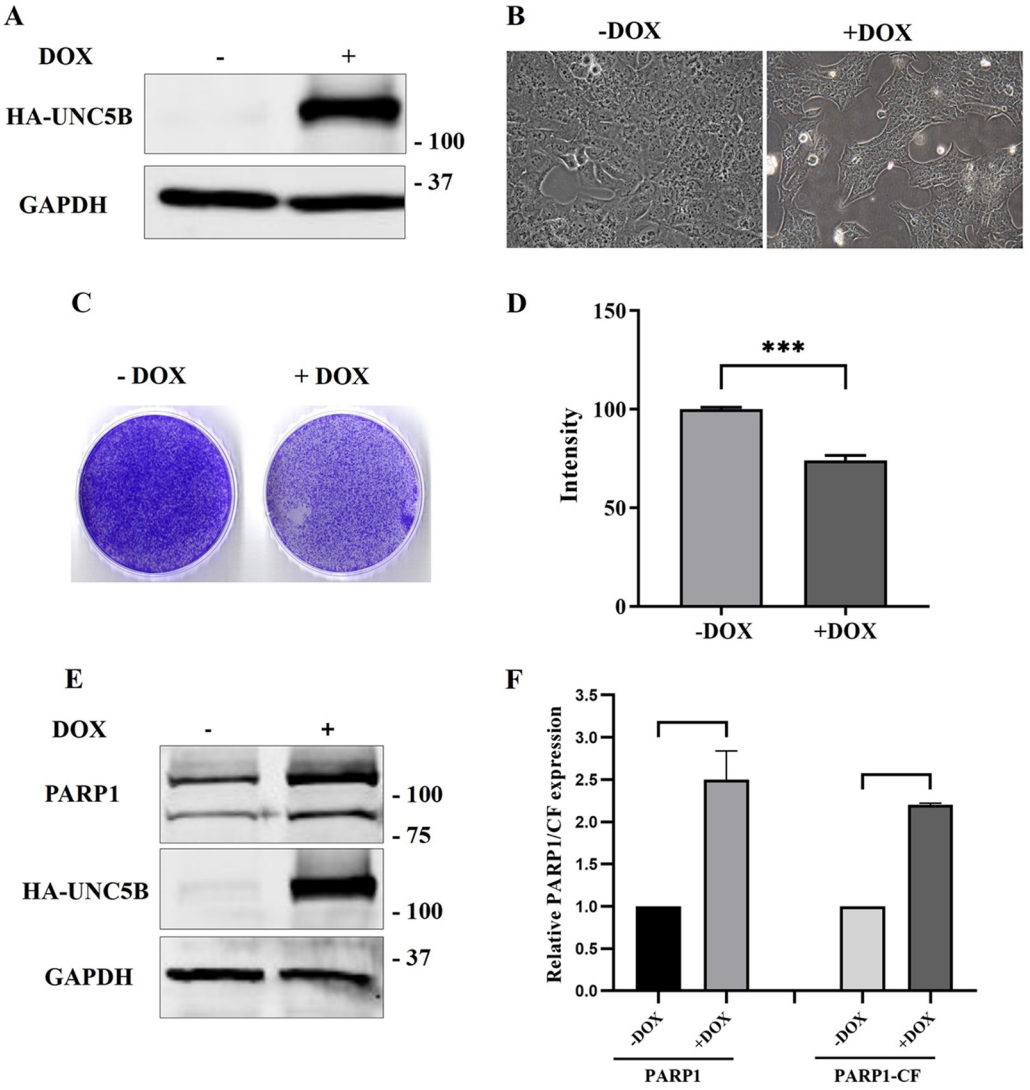

FIG 5 UNC5B expression induced apoptosis in U2OS cells. (A) UNC5B-U2OS stable cell line was induced with doxycycline (24 h), and cell lysates were blotted for UNC5B-HA expression using an anti-HA antibody. (B) Doxycycline was added to UNC5B-U2OS cells for 3 days, and cell morphology was determined by microscopy (×20 magnification). (C) UNC5B was induced in UNC5B-U2OS with doxycycline for 6 days, and adherent cells were stained with crystal violet solution. (D) In a separate experiment, UNC5B was induced in UNC5B-U2OS with doxycycline for 3 days, and stain was extracted and quantified at 595 nm; a graph was plotted for control (−DOX) versus induced (+DOX) cells. Values indicate means ± SEMs; $n = 3$ replicates. ***, $P = 0.0001$ to 0.001 (two-tailed unpaired Student's t test). (E) UNC5B was induced in UNC5B-U2OS with doxycycline, and cell lysates were blotted for PARP1 expression using an anti-PARP1 antibody. UNC5B expression was detected using an anti-HA antibody. (F) Graph representing relative PARP1 and PARP1 cleavage fragment (PARP1-CF) expression in UNC5B-U2OS cells under the −DOX and +DOX (48 h) conditions. PARP1 and PARP1-CF levels under the −DOX condition were arbitrarily taken as 1. Values indicate means ± SEMs; $n = 2$ biological replicates.

stabilizes UNC5B protein at the posttranslational level as well. The increase in UNC5B expression is dependent on PyST's ability to bind PP2A. Interestingly, our microarray results also revealed that, as opposed to other dependence receptors of the same family (i.e., UNC5A, -C, and -D or DCC), only UNC5B mRNA levels were increased. Interestingly, despite extensive structural similarities between dependence receptor members, PyST expression induced apoptosis specifically through the UNC5B receptor. UNC5B's ability to respond to mitotic abnormalities within the cells and trigger apoptotic signals is one area that certainly merits future investigations.

Using transient transfections in HEK 293T cells, we found that exogenous expression of PP2A-Aβ and -Cα (but not PP2A-Aα and -Cβ) as well as some regulatory B subunits, increases UNC5B protein levels. These results point to the role of specific PP2A subunits

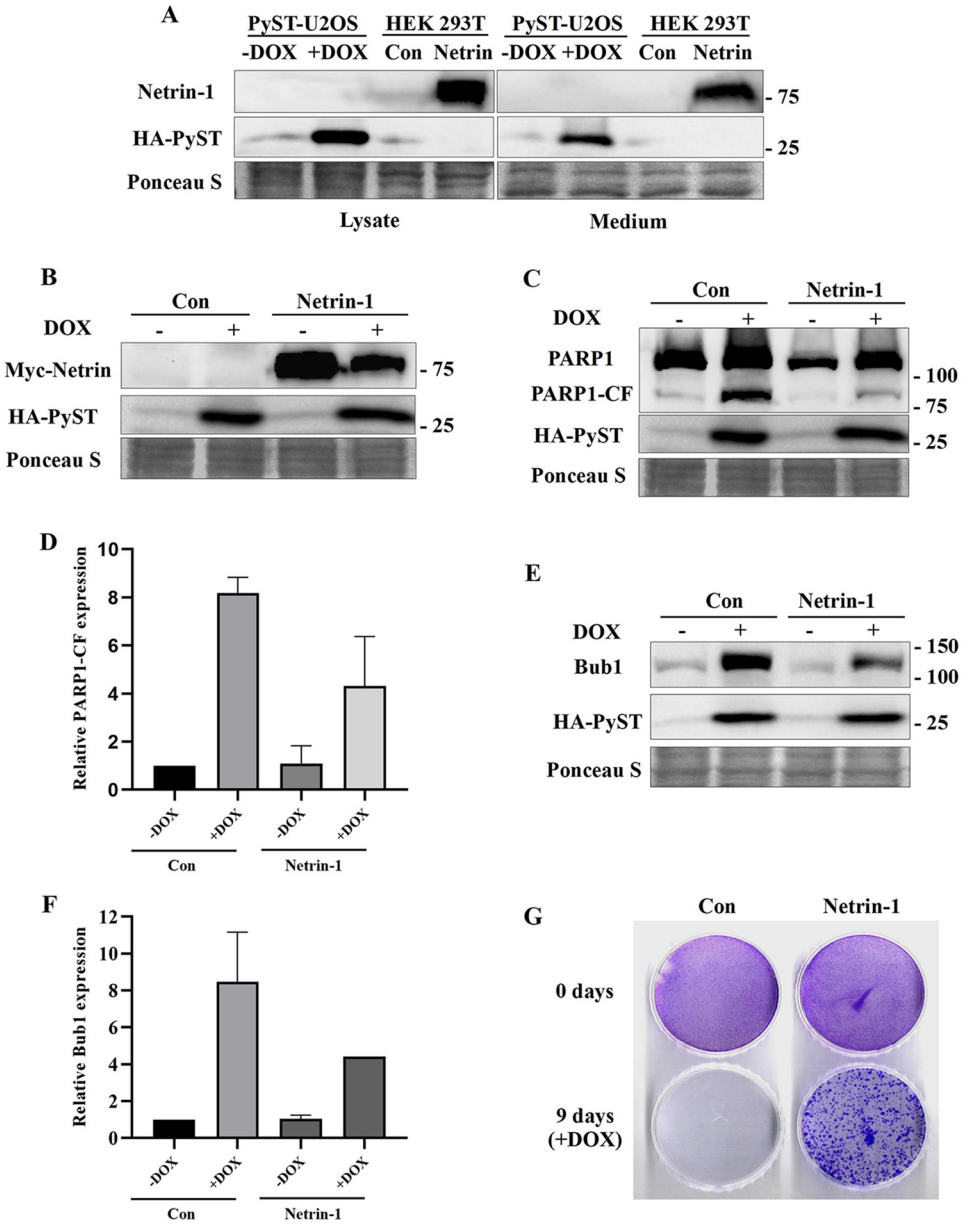

FIG 6 Expression of netrin-1 prevented UNC5B-mediated apoptosis: (A) Doxycycline was added to control and PyST-expressing U2OS cells for 30 h, and cell lysates and medium proteins were blotted for netrin-1 expression. HEK 293T cells transiently transfected with human netrin-1 were used as a positive control for detecting netrin-1 expression. (B) A U2OS cell line with a constitutive expression of netrin-1 was made in the PyST expression background. Cell lysates were blotted for Myc-netrin-1 expression using an anti-Myc antibody. (C) Control and netrin-1-expressing PyST-U2OS cells were grown in the presence of doxycycline for 30 h, and cell lysates were blotted for PARP1 expression. (D) Graph representing relative PARP1 cleavage fragment (PARP1-CF) expression in control and netrin-1-expressing PyST-U2OS cells under the −DOX and +DOX conditions. PARP1-CF levels in the control cells under the −DOX condition were arbitrarily taken as 1. Values indicate means ± SEMs; $n = 2$ biological replicates. (E) Control and netrin-1-expressing PyST-U2OS cells were grown in the presence of doxycycline (+DOX) for approximately 32 h, and cell lysates were blotted for Bub1 expression as a marker for mitosis. (F) Graph representing relative Bub1 expression in control and netrin-1-expressing PyST-U2OS cells under the −DOX and +DOX conditions. Bub1 level in the control cells under the −DOX condition was arbitrarily taken as 1. Values indicate means ± SEMs; $n = 2$ biological replicates. (G) Control and netrin-1-expressing PyST-U2OS cells were grown in the presence of doxycycline (+DOX) for several days, and adherent cells were stained with crystal violet solution to compare cell densities.

or holoenzyme complexes in the *regulation* of UNC5B-mediated apoptosis. These data are consistent with the findings of Mehlen's group (13), who have shown that PP2A-Aβ is needed to promote UNC5B-mediated apoptosis. Activation of the UNC5B pathway could also explain the tumor suppressor role of PP2A-Aβ. Such a role for PP2A-Aβ is

also supported by the findings of Hahn's group (26). They have shown that PP2A-Aβ, but not PP2A-Aα, dephosphorylates RalA GTPase, thereby inhibiting its oncogenic activity. They also showed evidence that PP2A-Aβ knockdown promotes cellular proliferation and anchorage independence in immortalized cells as well as tumor formation in mouse models. In contrast, overexpression of PP2A-Aβ reversed the tumorigenic phenotype of numerous cancerous cell lines and reduced the percentage of tumors in mice. It is quite possible that PP2A-Aβ might promote some of its tumor suppressor and proapoptotic functions through activation of the UNC5B pathway. Mutations as well deletions in PP2A-Aβ have been reported in numerous types of human cancers as well as in cancer cell lines (51–53). Quite interestingly, we found that the expression of PPME1, an endogenous PP2A inhibitor (46–50), was also downregulated by approximately 2-fold in PyST-expressing cells (Fig. 4J), which suggests that PP2A could be activated in these cells. This goes together with our results obtained with transient transfections showing that UNC5B protein amounts are stabilized in the presence of overexpressed PP2A subunits. Under stressful conditions, downregulation of PP2A inhibitors such as PPME1 might be a way of enhancing PP2A activity, which can contribute to UNC5B protein stabilization. The requirement of PP2A in this mechanism can be underscored by the fact that nocodazole and paclitaxel, well-known mitotic inhibitors that induce apoptosis, did not increase UNC5B levels in our experiments (Fig. 2H and I). These inhibitors affect the microtubule organization but not PP2A.

Our data support a mechanism in which PyST promotes an increase in UNC5B expression in a PP2A-dependent manner. We believe that changes in the subunit composition, localization, and activity of PP2A by PyST may affect some critical cellular activities, including mitotic regulation. PP2A is known to be extremely important at the entry as well as exit of mitosis (54–57). Deregulation of PP2A activity in actively dividing cells therefore leads to severe abnormalities during mitosis, as is clearly visible in PyST-expressing cells also, leading to the activation of the spindle assembly checkpoint (SAC). This is also supported by our data, as we have seen an upregulation of SAC markers (e.g., Bub1) in PyST-expressing cells. We believe that, due to prolonged SAC activation and mitotic arrest, these cells somehow enhance UNC5B transcription as well as posttranslational stabilization.

The tumor suppressor p53 is a known positive regulator of UNC5B transcription (10, 35), but our results show that the increase in UNC5B protein levels by PyST is p53 independent. We have previously shown and further confirmed in this study that PyST-induced apoptosis is independent of p53. Some other viral proteins such as E4orf4 of adenovirus also bind PP2A similarly to the polyomavirus T antigens and induce mitotic arrest and apoptosis in p53-independent manner (58). It is quite possible that in PyST-expressing cell lines, some transcriptional regulator(s) other than p53 may be involved in mRNA upregulation of UNC5B, while p53 may induce UNC5B under a different set of conditions. These findings are significant given the fact that the majority of cancers have nonfunctional p53 and hence are refractory to the conventional chemotherapeutic treatments that provoke p53 activation to induce apoptosis. Alternatively, such tumors may possibly be targeted for apoptosis in a p53-independent manner involving the activation of UNC5B or another such pathway(s) or regulators such as PP2A. Since PyST by itself does not have any intrinsic transcriptional activity, it must increase UNC5B expression by affecting some cellular transcriptional factor(s) other than p53. Since numerous transcriptional factors are regulated by their phosphorylation-dephosphorylation mechanisms, PP2A could play its role by promoting their dephosphorylated state. Identification of such transcriptional factor(s) would thus be of considerable clinical significance in the treatment of p53 mutant tumors.

A more serious point of concern is that netrin-1 expression is surprisingly increased when cells/tumors are treated with conventional chemotherapeutic agents such as doxorubicin, paclitaxel, 5-fluorouracil (5FU), cisplatin, etc. (59). Paradoxically, these drugs increase the expression of both netrin-1 and its receptors through the activation of p53, thus promoting cell survival and growth. The netrin-1/UNC5B pathway plays a

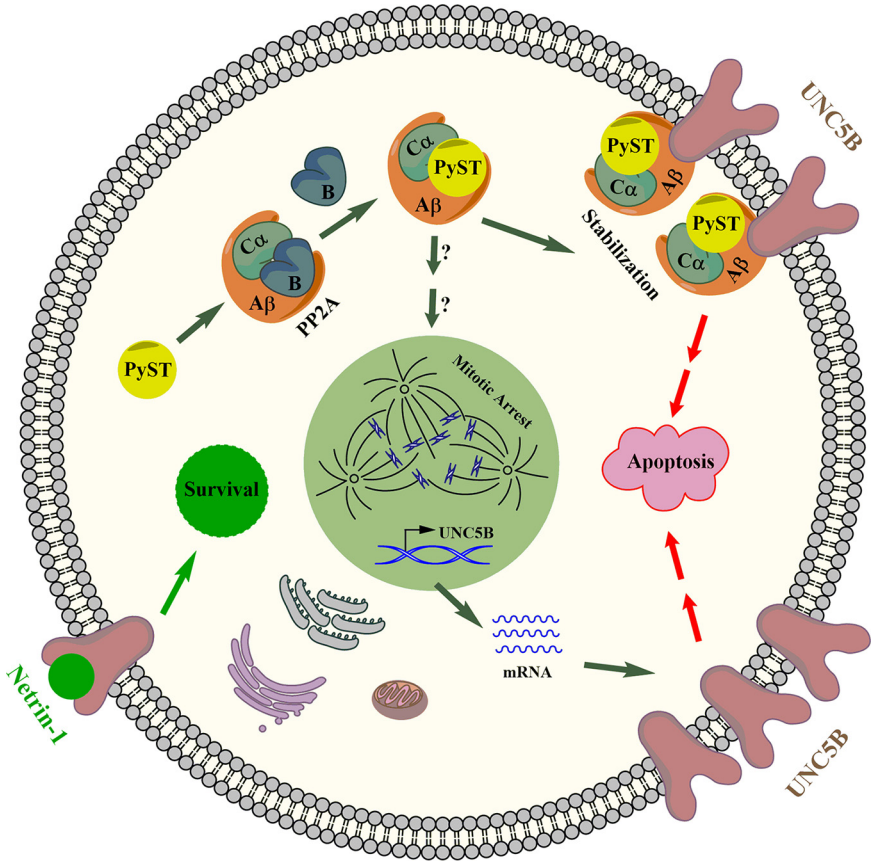

FIG 7 Proposed model of PyST-induced apoptosis through the netrin-UNC5B mechanism. PyST upregulates UNC5B expression both at mRNA and protein (posttranslational) levels. Increase in UNC5B stabilization occurs as a result of displacement of particular B subunit(s) of PP2A by PyST and hence change in PP2A activity. This promotes mitotic catastrophe, as PP2A has a very important role in the regulation of mitosis. As a result of PP2A-dependent mitotic arrest, UNC5B is upregulated through an unknown mechanism. Simultaneously, increased UNC5B expression through enhanced transcription also occurs as a result of numerous mitotic abnormalities, the details of which are not yet fully understood. As UNC5B is unbound by the ligand, it promotes cells death. However, when netrin-1 is expressed, it inhibits UNC5B-mediated apoptosis and promotes cell survival.

crucial role in the angiogenesis process as well, thus favoring tumor growth (17). Disruption of this signaling pathway has thus been proposed to be a promising strategy for the treatment of cancer, with many advantages. One is that this pathway is involved in numerous cancers and also at different levels, affecting both apoptosis and angiogenesis. Second is that these proteins are expressed extracellularly, thus making them accessible to agents such as antibodies, decoy proteins, and drugs, thus reducing the toxicity burden. A promising treatment that involves disruption of netrin-1 binding to UNC5B, so as to inhibit the prosurvival signaling, has already been designed. In such cases, blocking netrin-1 binding to UNC5B using an antibody against netrin-1 or molecules such as TRAP-netrin^{UNC5A} and Trap-netrin^{DCC} as proposed by Mehlen's group (18, 59, 60) may be quite effective in overcoming resistance promoted by netrin-1 binding to UNC5B. These antibodies are already in clinical trials and assume great significance in the treatment of at least some types of cancers such as colorectal cancer (19), breast cancer (21), and neuroblastomas (20), where netrin-1 expression is quite high.

Figure 7 depicts a simplified model of this pathway in light of the existing knowledge and our findings. However, more work needs to be undertaken to fill the obvious gaps and fully understand the PP2A/netrin-UNC5B pathway and its role in apoptosis.

MATERIALS AND METHODS

Reagents. Antibodies against UNC5B, PARP1, p53, and GAPDH and secondary antibodies (horseradish peroxidase [HRP]-conjugated and IRDye 680 and 800) were purchased from Cell Signaling Technology, USA). Anti-HA and anti-Flag antibodies, cycloheximide, okadaic acid, doxycycline, propidium iodide, polybrene, crystal violet, and protease and phosphatase inhibitors (Complete, Roche) were obtained from Sigma-Aldrich. All cell culture reagents, including Dulbecco's modified Eagle's medium (DMEM), fetal calf serum (FCS), and antibiotics were purchased from Invitrogen/Thermo Fisher Scientific, USA. Reagents for cDNA synthesis (iScript cDNA synthesis kit), a quantitative real-time PCR master mix (iTaq Universal SYBR Green supermix), a protein estimation kit (Bradford reagent), and nitrocellulose membranes were purchased from Bio-Rad Laboratories, USA. Reagents for cell cycle analysis were purchased from BD Biosciences, USA. Inhibitors such as etoposide, aphidicolin, hydroxyurea, and nocodazole were obtained from EMD Biosciences/Thermo Fisher Scientific, USA. Primers were obtained from Integrated DNA Technologies (IDT), Singapore. Polyethyleneimine (PEI) was obtained from Polysciences, USA.

Cell lines. 293T, U2OS, Phoenix, HeLa, A549, FT, and inducible pTREX-PyST-HA-FLAG U2OS cells were provided by Thomas M. Roberts. C6 rat glioma, HBL glioma cell lines, and SW480 cell lines were obtained from Firdous Khanday, University of Kashmir. All cell lines were cultured in DMEM, 10% FBS, and appropriate antibiotics (penicillin and streptomycin) and at 37°C with 5% CO_2.

Plasmid constructs. pCDNA-topo-UNC5B-HA (the HA tag is at the C terminus of UNC5B) and pGNET1-myc constructs were kindly provided by Patrick Mehlen (CRCL, Lyon, France). Gateway cloning was used to make a UNC5B-expressing construct. For Gateway cloning, primers were designed to have flanking attB sites required for recombination. Gateway cloning is a two-step cloning procedure involving BP and LR reactions. The gene of interest was amplified from pCDNA-topo-UNC5B-HA using primers with flanking attB sites. The BP reaction was then carried out to transfer the gene of interest to the entry vector (pDONR-223), which resulted in the generation of donor vector containing the gene of interest (pDONR-223-UNC5B). The BP reaction was followed by the LR reaction, which transferred the insert to the destination vector (pLenti-CMV-TO-Neo-DEST; Addgene). pLenti-CMV-TO-Neo-DEST is a lentiviral mammalian expression vector which requires a TetR (tetracycline repressor)-expressing construct to function in an inducible manner. The UNC5B-expressing construct named pLenti-CMV-TO-Neo-UNC5B was used to generate a stable cell line with inducible expression of UNC5B. The primers used for gateway cloning were UNC5B-forward, GGG GAC AAG TTT GTA CAA AAA AGC AGG CTA CCA TGA GGG CCC GGA GCG G, and HA-reverse, GGG GAC CAC TTT GTA CAA GAA AGC TGG GTC TAT GCA TAA TCC GGC ACA TCA TAC GG. Netrin-1 was cloned from the pGNET1-myc vector to pWZL-BLAST using common restriction enzyme sites for EcoRI and XhoI in these vectors. pWZL-BLAST is a retroviral mammalian expression vector and is constitutive. The netrin-1-expressing construct named pWZL-BLAST-Net1 was used to generate a stable cell line with a constitutive expression of netrin-1. A Pinco-GFP construct was used as transfection control (31, 61).

Dominant negative p53 (pWZL-DNp53DD) was obtained from Jean Zhao, DFCI, Harvard University. PyST-HA-FLAG was previously cloned in inducible pTREX-puro vector (designated pTREX-PyST-HA-FLAG). Both these plasmids have been described previously (32). The wild-type PyST-HA-FLAG gene and its tagged mutants HSP− (D44N) and PP2A− (BC1075) were cloned in pCDNA3.1 in our laboratory. The D44N construct has a J domain in which the HPDKGG motif has been mutated at residue 44, and BC1075 is a PP2A binding mutant in which cysteine 142 is mutated to tyrosine. These mutations were previously reported by other groups (31, 40–45). PP2A constructs were provided by Thomas M. Roberts. Flag-tagged versions of the PP2A constructs were cloned in the pLenti-CMV-BLAST vector (Addgene) also in our laboratory, using standard cloning procedures. For experiments needing transfection control, the Pinco-GFP construct was used.

Cell culture and transient transfections. U2OS cells and HEK 293T cells were grown in Dulbecco's modified Eagle's medium (DMEM) medium containing 10% fetal bovine serum (FBS) and antibiotics (penicillin and streptomycin) at 37°C and 5% CO_2. Cells were split 1 day prior to transfection so as to have approximately 50% confluence at the time of transfection. Polyethyleneimine solution (PEI) (stock concentration, 1 mg/ml) was used as the transfection reagent. Plasmid DNA and a PEI solution were added to 400 μl of DMEM in a 1 μg/3μl ratio, mixed, and incubated at room temperature for approximately 15 min before being added dropwise to culture plates. The plates were kept in the incubator overnight. The next day, the medium was changed and cells were harvested at approximately 48 h.

Viral transductions. For retroviral/lentiviral transductions, packaging cells were grown in 6-cm plates. Phoenix and FT packaging cells (packaging constructs were still transfected for supplementation) were used for retro- and lentiviral infections, respectively. Retroviral expression plasmids (3 μg) were mixed in DMEM with viral packaging plasmids Gag-Pol (1 μg) and VSVG (1 μg). For lentiviral transductions, lentiviral expression plasmids (2.5 μg) were mixed in DMEM with lentiviral packaging plasmids ΔR (2.25 μg) and VSVG (0.25 μg). As for the transient transfections, polyethyleneimine (PEI) was used as the transfection reagent. The medium was changed the next day, viral titers were collected at 48 h and 72 h, and the virus was used to infect host cells for 4 to 6 h on consecutive days. Polybrene (8 μg/ml) was used as a cell binding agent for virus. Cells were grown for 1 day after infections and were subsequently selected in the presence of appropriate selection drugs for 5 to 7 days until the selections were completed.

Microarray analysis. Total cellular RNA was isolated by the TRIzol method (Invitrogen) from pTREX-PyST-HA-FLAG U2OS cell lines from control (−DOX) and PyST-expressing cells (+DOX, 20 h) in triplicates. RNA was isolated at the same time from cells grown in three separate 6-cm plates each for control (−DOX) and PyST-expressing cells (+DOX). At this time point, extensive cell rounding, which indicates mitotic arrest, was clearly visible. The samples were further purified using the RNeasy Miniprep

kit (Qiagen). The quantity and quality of the samples were further confirmed by spectrometry and running on an agarose gel, respectively. RNA samples were then subjected to microarray analysis at DFCI, Harvard Medical School microarray core facility. Microarray experiments were conducted for technical triplicates for both the samples, using whole-genome Affymetrix human genome U133 Plus 2.0 (HG-U133_Plus_2) chips. Genes having log2 fold or more fold changes in expression were considered for further analyses and for generating the heat map. Gene set enrichment analysis (GSEA) was carried out using GSEA (V4.0.3) (https://www.gsea-msigdb.org/gsea/index.jsp) (62).

Western blotting. Cells were lysed in NP-40 lysis buffer (Tris-Cl, 50 mM; NaCl, 150 mM; glycerol, 10%; SDS, 0.1%; NP-40, 1%; EDTA, 2 mM) containing protease and phosphatase inhibitors (Complete, Roche). Cell lysates were centrifuged, and supernatants were mixed with 5× sample buffer (0.5 M Tris-Cl [pH 6.8], 1.25 g SDS, 0.0025 g bromophenol blue), followed by boiling at 100°C. Protein estimations were conducted by using the Bradford assay (Bio-Rad Laboratories). Equal amounts of proteins were loaded on SDS-PAGE gels and then blotted on nitrocellulose membranes. Membranes were blocked with 3% milk in 1× TBS-T (8 g of NaCl, 0.2 g of KCl, 0.3 g of Tris-Cl for 1 liter), incubated with primary antibody solution at 4°C overnight, washed with TBS-T, and then incubated with secondary antibodies (DyLight 680 and DyLight 800 for infrared detection or HRP-conjugated antibodies for chemiluminescence). The blots were then detected using LI-COR Odyssey (for infrared detection) or ChemiDoc MP (Bio-Rad Laboratories; for chemiluminescence). Quantifications for all Western blots were carried out by densitometric analysis using Image Studio Lite ver 5.2 (LI-COR Biosciences). Normalization was to total protein detected by Ponceau S staining, to an internal loading control, or to a coexpressing protein depending on the experiment. For total protein quantification, the whole lane as detected by Ponceau S staining was quantified using Image Studio Lite software. Data were analyzed using GraphPad Prism software.

Cycloheximide chase assay. HEK 293T cells were split in 60-mm dishes. The next day, they were transfected with 1 μg of pCDNA-topo-UNC5B and 2 μg of pCDNA3.1-PyST-HA-FLAG constructs. After approximately 40 h posttransfection, cycloheximide was added at a concentration of 25 μg/ml for different time periods (3, 6, 9, and 12 h). Cell lysates were obtained using cell NP-40 lysis buffer containing protease and phosphatase inhibitors and subjected to Western blotting as described above. Data obtained after densitometry analysis using Image Studio Lite ver 5.2 (LI-COR Biosciences) were used for making graphs for comparing protein amounts from different samples. Statistical analysis was performed using GraphPad Prism software.

Flow cytometry. Equal numbers of cells from different cell lines were grown in 60-mm dishes. At the required time points, medium was collected in 15-ml tubes. Cells were washed with phosphate-buffered saline (PBS) containing 0.1% EDTA, which was also collected. PBS-EDTA was then added to the plates, and the plates were incubated at 37°C for 5 to 10 min. Cells were collected and pelleted at 1,000 × *g* for 5 min followed by washing in PBS-serum (1% serum) and centrifuged again at 1,000 × *g*. Cells were then resuspended in 0.5 ml PBS. Next, 5 ml ethanol was added dropwise, and the cell mixtures were vortexed to prevent cell clumping. Cells were then stored at −20°C for at least overnight. Prior to FACS analysis, fixed samples were spun down at 1,000 × *g* for 5 min, washed with PBS/serum, and then resuspended in RNase/propidium iodide solution (50 μg/ml propidium iodide, 10 mM Tris [pH 7.5], 5 mM $MgCl_2$, and 20 μg/ml RNase A). Samples were acquired in a BD FACSVerse machine and analyzed by BD FACSuite software. GraphPad Prism software was used for statistical analysis of our data.

Crystal violet staining. This method was used to compare cell densities among different samples. Equal numbers of cells from different cell lines were initially seeded in different plates and were grown for the required time periods. At the time of terminating the experiments, cells were washed with 1× PBS, fixed with methanol for 10 min, and then stained with 0.5% crystal violet dye for 10 to 15 min. The stain was subsequently discarded, and plates were washed with distilled water and allowed to dry. For quantification purposes, plates were destained by using a 10% acetic acid solution. The destained solutions were used for measuring absorbance at 595 nm. Data were analyzed using GraphPad Prism software.

Real-time quantitative PCR. Cells were grown for the required time periods and harvested. RNA was isolated by the TRIzol extraction method (Invitrogen) and quantified by a NanoDrop. cDNA synthesis was conducted using a Bio-Rad iScript cDNA synthesis kit. Real-time quantitative PCR (RT-qPCR) was performed using iTaq Universal SYBR green supermix. CAG GGC AAG TTC TAC GAG AT forward and TGG TCC AGC AGG ATG TGA reverse primers were used for UNC5B amplification, and TTA GTT GCG TTA CAC CCT TTC forward and ACC TTC ACC GTT CCA GTT T reverse primers were used for actin amplification. Normalized gene expression ($\Delta\Delta C_q$) was carried out by Bio-Rad CFX Manager. Normalization was performed by using actin as control.

Immunofluorescence. Cells were grown on coverslips overnight, given appropriate treatment, and washed with PBS. This was followed by fixation in 4% paraformaldehyde in PBS for 15 min at room temperature. Cells were washed with PBS, permeabilized in 100% methanol at −20°C for 10 min, and washed in PBS for 5 min. The samples were blocked in 3% bovine serum albumin (BSA) in PBS-Triton (1× PBS, 0.3% Triton X-100) for 1 h, followed by incubation in an appropriate primary antibody (anti-UNC5B or anti-tubulin; 1:100 dilution) overnight at 4°C. The samples were then rinsed three times in PBS for 5 min each. This was followed by incubation in secondary antibody (1:3,000 to 1:5,000 dilution) at room temperature for approximately 1 h and rinsing in PBS three times for 5 min each. Coverslips were finally mounted on glass slides on which DAPI-containing antifade solution was applied, and the samples were observed by using an immunofluorescence microscope. Pictures were taken at ×63 magnification with a Carl Zeiss Axio Observer 7.0 microscope using apotome.

Data availability. The microarray data discussed in this paper are available in NCBI's Gene Expression Omnibus (GEO) under accession number GSE149525.

ACKNOWLEDGMENTS

This work was supported by the Department of Biotechnology (DBT), Government of India, through the following grants: Ramalingaswami Fellowship, BT/PR2283/AGR/36/692/2011, and BT/PR5743/BRB/10/1100/2012. Work in the lab of T.M.R was supported by a grant from the NIH: P01 CA203655. This work was also supported by the Department of Science and Technology (DST), Government of India, through their FIST grants to the Department of Biochemistry, University of Kashmir. The Department of Science and Technology (DST), India, awarded DST INSPIRE fellowships to Sameer Ahmed Bhat, Zarka Sarwar, and Syed Qaaifah Gillani. CSIR and UGC, India, awarded fellowships to Misbah Un Nisa, Irfana Reshi, and Nusrat Nabi.

We thank Patrick Mehlen for providing the UNC5B and netrin-1 constructs used in this study and Shakil Wani, Zahid Kashoo, and their colleagues for allowing us to carry out the FACS analysis in their laboratory at the SKUAST campus, Shuhama, Srinagar. We also thank Brian Schaffhausen, Tufts University, USA, for reviewing the manuscript and providing critical comments.

T.M.R. participates on the corporate boards of the following companies: iKang Healthcare and Crimson BioPharm. In addition, T.M.R. has a consulting relationship with Novartis and is a founder and member of the corporate boards of Crimson Biotech and Geode Therapeutics.

S.A.B. and S.A. designed the experiments, analyzed data, and wrote the manuscript. Z.S., S.Q.G., I.R., M.U.N., and N.N. helped with the experiments. K.M.F. helped with data interpretation and the experimental plan. S.X. helped with analyzing and interpreting the microarray data, obtaining the heat map, and planning the real-time qPCR experiments. T.M.R helped plan experiments, analyze data, and critically review the manuscript.

REFERENCES

1. Bagri A, Ashkenazi A. 2010. UNCovering the molecular machinery of dependence receptor signaling. Mol Cell 40:851–853. https://doi.org/10.1016/j.molcel.2010.12.015.
2. Arakawa H. 2004. Netrin-1 and its receptors in tumorigenesis. Nat Rev Cancer 4:978–987. https://doi.org/10.1038/nrc1504.
3. Goldschneider D, Mehlen P. 2010. Dependence receptors: a new paradigm in cell signaling and cancer therapy. Oncogene 29:1865–1882. https://doi.org/10.1038/onc.2010.13.
4. Ko SY, Dass CR, Nurgali K. 2012. Netrin-1 in the developing enteric nervous system and colorectal cancer. Trends Mol Med 18:544–554. https://doi.org/10.1016/j.molmed.2012.07.001.
5. Lai Wing Sun K, Correia JP, Kennedy TE. 2011. Netrins: versatile extracellular cues with diverse functions. Development 138:2153–2169. https://doi.org/10.1242/dev.044529.
6. Wang R, Wei Z, Jin H, Wu H, Yu C, Wen W, Chan L-N, Wen Z, Zhang M. 2009. Autoinhibition of UNC5b revealed by the cytoplasmic domain structure of the receptor. Mol Cell 33:692–703. https://doi.org/10.1016/j.molcel.2009.02.016.
7. Llambi F, Causeret F, Bloch-Gallego E, Mehlen P. 2001. Netrin-1 acts as a survival factor via its receptors UNC5H and DCC. EMBO J 20:2715–2722. https://doi.org/10.1093/emboj/20.11.2715.
8. Hayano Y, Sasaki K, Ohmura N, Takemoto M, Maeda Y, Yamashita T, Hata Y, Kitada K, Yamamoto N. 2014. Netrin-4 regulates thalamocortical axon branching in an activity-dependent fashion. Proc Natl Acad Sci U S A 111:15226–15231. https://doi.org/10.1073/pnas.1402095111.
9. Lejmi E, Bouras I, Camelo S, Roumieux M, Minet N, Leré-Déan C, Merkulova-Rainon T, Autret G, Vayssettes C, Clement O, Plouët J, Leconte L. 2014. Netrin-4 promotes mural cell adhesion and recruitment to endothelial cells. Vasc Cell 6:1. https://doi.org/10.1186/2045-824X-6-1.
10. Tanikawa C, Matsuda K, Fukuda S, Nakamura Y, Arakawa H. 2003. p53RDL1 regulates p53-dependent apoptosis. Nat Cell Biol 5:216–223. https://doi.org/10.1038/ncb943.
11. Wang H, Copeland NG, Gilbert DJ, Jenkins NA, Tessier-Lavigne M. 1999. Netrin-3, a mouse homolog of human NTN2L, is highly expressed in sensory ganglia and shows differential binding to netrin receptors. J Neurosci 19:4938–4947. https://doi.org/10.1523/JNEUROSCI.19-12-04938.1999.
12. Cirulli V, Yebra M. 2007. Netrins: beyond the brain. Nat Rev Mol Cell Biol 8:296–306. https://doi.org/10.1038/nrm2142.
13. Guenebeaud C, Goldschneider D, Castets M, Guix C, Chazot G, Delloye-Bourgeois C, Eisenberg-Lerner A, Shohat G, Zhang M, Laudet V, Kimchi A, Bernet A, Mehlen P. 2010. The dependence receptor UNC5H2/B triggers apoptosis via PP2A-mediated dephosphorylation of DAP kinase. Mol Cell 40:863–876. https://doi.org/10.1016/j.molcel.2010.11.021.
14. Tang X, Jang S-W, Okada M, Chan C-B, Feng Y, Liu Y, Luo S-W, Hong Y, Rama N, Xiong W-C, Mehlen P, Ye K. 2008. Netrin-1 mediates neuronal survival through PIKE-L interaction with the dependence receptor UNC5B. Nat Cell Biol 10:698–706. https://doi.org/10.1038/ncb1732.
15. Furne C, Rama N, Corset V, Chedotal A, Mehlen P. 2008. Netrin-1 is a survival factor during commissural neuron navigation. Proc Natl Acad Sci U S A 105:14465–14470. https://doi.org/10.1073/pnas.0803645105.
16. Mehlen P, Delloye-Bourgeois C, Chédotal A. 2011. Novel roles for slits and netrins: axon guidance cues as anticancer targets? Nat Rev Cancer 11:188–197. https://doi.org/10.1038/nrc3005.
17. Koch AW, Mathivet T, Larrivee B, Tong RK, Kowalski J, Pibouin-Fragner L, Bouvree K, Stawicki S, Nicholes K, Rathore N, Scales SJ, Luis E, del Toro R, Freitas C, Breant C, Michaud A, Corvol P, Thomas JL, Wu Y, Peale F, Watts RJ, Tessier-Lavigne M, Bagri A, Eichmann A. 2011. Robo4 maintains vessel integrity and inhibits angiogenesis by interacting with UNC5B. Dev Cell 20:33–46. https://doi.org/10.1016/j.devcel.2010.12.001.
18. Mehlen P, Guenebeaud C. 2010. Netrin-1 and its dependence receptors as original targets for cancer therapy. Curr Opin Oncol 22:46–54. https://doi.org/10.1097/CCO.0b013e328333dcd1.
19. Mazelin L, Bernet A, Bonod-Bidaud C, Pays L, Arnaud S, Gespach C, Bredesen DE, Scoazec JY, Mehlen P. 2004. Netrin-1 controls colorectal tumorigenesis by regulating apoptosis. Nature 431:80–84. https://doi.org/10.1038/nature02788.
20. Delloye-Bourgeois C, Fitamant J, Paradisi A, Cappellen D, Douc-Rasy S, Raquin M-A, Stupack D, Nakagawara A, Rousseau R, Combaret V, Puisieux A, Valteau-Couanet D, Bénard J, Bernet A, Mehlen P. 2009. Netrin-1 acts as a survival factor for aggressive neuroblastoma. J Exp Med 206:833–847. https://doi.org/10.1084/jem.20082299.
21. Fitamant J, Guenebeaud C, Coissieux MM, Guix C, Treilleux I, Scoazec JY,

Bachelot T, Bernet A, Mehlen P. 2008. Netrin-1 expression confers a selective advantage for tumor cell survival in metastatic breast cancer. Proc Natl Acad Sci U S A 105:4850–4855. https://doi.org/10.1073/pnas.0709810105.
22. Thiebault K, Mazelin L, Pays L, Llambi F, Joly M-O, Scoazec J-Y, Saurin J-C, Romeo G, Mehlen P. 2003. The netrin-1 receptors UNC5H are putative tumor suppressors controlling cell death commitment. Proc Natl Acad Sci U S A 100:4173–4178. https://doi.org/10.1073/pnas.0738063100.
23. Bhat SA, Gurtoo S, Deolankar SC, Fazili KM, Advani J, Shetty R, Prasad TSK, Andrabi S, Subbannayya Y. 2019. A network map of netrin receptor UNC5B-mediated signaling. J Cell Commun Signal 13:121–127. https://doi.org/10.1007/s12079-018-0485-z.
24. Seshacharyulu P, Pandey P, Datta K, Batra SK. 2013. Phosphatase: PP2A structural importance, regulation and its aberrant expression in cancer. Cancer Lett 335:9–18. https://doi.org/10.1016/j.canlet.2013.02.036.
25. Junttila MR, Puustinen P, Niemelä M, Ahola R, Arnold H, Böttzauw T, Ala-Aho R, Nielsen C, Ivaska J, Taya Y, Lu S-L, Lin S, Chan EKL, Wang X-J, Grènman R, Kast J, Kallunki T, Sears R, Kähäri V-M, Westermarck J. 2007. CIP2A inhibits PP2A in human malignancies. Cell 130:51–62. https://doi.org/10.1016/j.cell.2007.04.044.
26. Sablina AA, Chen W, Arroyo JD, Corral L, Hector M, Bulmer SE, DeCaprio JA, Hahn WC. 2007. The tumor suppressor PP2A Abeta regulates the RalA GTPase. Cell 129:969–982. https://doi.org/10.1016/j.cell.2007.03.047.
27. Shi Y. 2009. Serine/threonine phosphatases: mechanism through structure. Cell 139:468–484. https://doi.org/10.1016/j.cell.2009.10.006.
28. Pallas DC, Shahrik LK, Martin BL, Jaspers S, Miller TB, Brautigan DL, Roberts TM. 1990. Polyoma small and middle T antigens and SV40 small T antigen form stable complexes with protein phosphatase 2A. Cell 60:167–176. https://doi.org/10.1016/0092-8674(90)90726-u.
29. Arroyo JD, Hahn WC. 2005. Involvement of PP2A in viral and cellular transformation. Oncogene 24:7746–7755. https://doi.org/10.1038/sj.onc.1209038.
30. Kleinberger T, Shenk T. 1993. Adenovirus E4orf4 protein binds to protein phosphatase 2A, and the complex down regulates E1A-enhanced *junB* transcription. J Virol 67:7556–7560. https://doi.org/10.1128/JVI.67.12.7556-7560.1993.
31. Andrabi S, Gjoerup OV, Kean JA, Roberts TM, Schaffhausen B. 2007. Protein phosphatase 2A regulates life and death decisions via Akt in a context-dependent manner. Proc Natl Acad Sci U S A 104:19011–19016. https://doi.org/10.1073/pnas.0706696104.
32. Pores Fernando AT, Andrabi S, Cizmecioglu O, Zhu C, Livingston DM, Higgins JMG, Schaffhausen BS, Roberts TM. 2015. Polyoma small T antigen triggers cell death via mitotic catastrophe. Oncogene 34:2483–2492. https://doi.org/10.1038/onc.2014.192.
33. Reshi I, Sarwar Z, Bhat SA, Gillani SQ, Shah M, Fazili KM, Andrabi S. 2018. Polyoma small T upregulates the expression of cytoskeletal proteins in mammalian cells during mitosis. Int J Biol Macromol 107:2279–2284. https://doi.org/10.1016/j.ijbiomac.2017.10.110.
34. Blajeski AL, Phan VA, Kottke TJ, Kaufmann SH. 2002. G_1 and G_2 cell-cycle arrest following microtubule depolymerization in human breast cancer cells. J Clin Invest 110:91–99. https://doi.org/10.1172/JCI13275.
35. He K, Jang SW, Joshi J, Yoo MH, Ye K. 2011. Akt-phosphorylated PIKE-A inhibits UNC5B-induced apoptosis in cancer cell lines in a p53-dependent manner. Mol Biol Cell 22:1943–1954. https://doi.org/10.1091/mbc.E10-11-0923.
36. Chen YL, Eriksson S, Chang ZF. 2010. Regulation and functional contribution of thymidine kinase 1 in repair of DNA damage. J Biol Chem 285:27327–27335. https://doi.org/10.1074/jbc.M110.137042.
37. Marusyk A, Wheeler LJ, Mathews CK, DeGregori J. 2007. p53 mediates senescence-like arrest induced by chronic replicational stress. Mol Cell Biol 27:5336–5351. https://doi.org/10.1128/MCB.01316-06.
38. Llambi F, Lourenco FC, Gozuacik D, Guix C, Pays L, Del Rio G, Kimchi A, Mehlen P. 2005. The dependence receptor UNC5H2 mediates apoptosis through DAP-kinase. EMBO J 24:1192–1201. https://doi.org/10.1038/sj.emboj.7600584.
39. Andrabi S, Hwang JH, Choe JK, Roberts TM, Schaffhausen BS. 2011. Comparisons between murine polyomavirus and simian virus 40 show significant differences in small T antigen function. J Virol 85:10649–10658. https://doi.org/10.1128/JVI.05034-11.
40. Martens I, Nilsson SA, Linder S, Magnusson G. 1989. Mutational analysis of polyomavirus small-T-antigen functions in productive infection and in transformation. J Virol 63:2126–2133. https://doi.org/10.1128/JVI.63.5.2126-2133.1989.
41. Campbell KS, Auger KR, Hemmings BA, Roberts TM, Pallas DC. 1995. Identification of regions in polyomavirus middle T and small T antigens important for association with protein phosphatase 2A. J Virol 69:3721–3728. https://doi.org/10.1128/JVI.69.6.3721-3728.1995.
42. Brodsky JL, Pipas JM. 1998. Polyomavirus T antigens: molecular chaperones for multiprotein complexes. J Virol 72:5329–5334. https://doi.org/10.1128/JVI.72.7.5329-5334.1998.
43. Campbell KS, Mullane KP, Aksoy IA, Stubdal H, Zalvide J, Pipas JM, Silver PA, Roberts TM, Schaffhausen BS, DeCaprio JA. 1997. DnaJ/hsp40 chaperone domain of SV40 large T antigen promotes efficient viral DNA replication. Genes Dev 11:1098–1110. https://doi.org/10.1101/gad.11.9.1098.
44. Genevaux P, Lang F, Schwager F, Vartikar JV, Rundell K, Pipas JM, Georgopoulos C, Kelley WL. 2003. Simian virus 40 T antigens and J domains: analysis of Hsp40 cochaperone functions in *Escherichia coli*. J Virol 77:10706–10713. https://doi.org/10.1128/jvi.77.19.10706-10713.2003.
45. Sullivan CS, Pipas JM. 2002. T antigens of simian virus 40: molecular chaperones for viral replication and tumorigenesis. Microbiol Mol Biol Rev 66:179–202. https://doi.org/10.1128/mmbr.66.2.179-202.2002.
46. Puustinen P, Junttila MR, Vanhatupa S, Sablina AA, Hector ME, Teittinen K, Raheem O, Ketola K, Lin S, Kast J, Haapasalo H, Hahn WC, Westermarck J. 2009. PME-1 protects extracellular signal-regulated kinase pathway activity from protein phosphatase 2A-mediated inactivation in human malignant glioma. Cancer Res 69:2870–2877. https://doi.org/10.1158/0008-5472.CAN-08-2760.
47. Wandzioch E, Pusey M, Werda A, Bail S, Bhaskar A, Nestor M, Yang JJ, Rice LM. 2014. PME-1 modulates protein phosphatase 2A activity to promote the malignant phenotype of endometrial cancer cells. Cancer Res 74:4295–4305. https://doi.org/10.1158/0008-5472.CAN-13-3130.
48. Kaur A, Elzagheid A, Birkman EM, Avoranta T, Kytola V, Korkeila E, Syrjanen K, Westermarck J, Sundstrom J. 2015. Protein phosphatase methylesterase-1 (PME-1) expression predicts a favorable clinical outcome in colorectal cancer. Cancer Med 4:1798–1808. https://doi.org/10.1002/cam4.541.
49. Kaur A, Denisova OV, Qiao X, Jumppanen M, Peuhu E, Ahmed SU, Raheem O, Haapasalo H, Eriksson J, Chalmers AJ, Laakkonen P, Westermarck J. 2016. PP2A inhibitor PME-1 drives kinase inhibitor resistance in glioma cells. Cancer Res 76:7001–7011. https://doi.org/10.1158/0008-5472.CAN-16-1134.
50. Kaur A, Westermarck J. 2016. Regulation of protein phosphatase 2A (PP2A) tumor suppressor function by PME-1. Biochem Soc Trans 44:1683–1693. https://doi.org/10.1042/BST20160161.
51. Ruediger R, Pham HT, Walter G. 2001. Alterations in protein phosphatase 2A subunit interaction in human carcinomas of the lung and colon with mutations in the A beta subunit gene. Oncogene 20:1892–1899. https://doi.org/10.1038/sj.onc.1204279.
52. Takagi Y, Futamura M, Yamaguchi K, Aoki S, Takahashi T, Saji S. 2000. Alterations of the PPP2R1B gene located at 11q23 in human colorectal cancers. Gut 47:268–271. https://doi.org/10.1136/gut.47.2.268.
53. Tamaki M, Goi T, Hirono Y, Katayama K, Yamaguchi A. 2004. PPP2R1B gene alterations inhibit interaction of PP2A-Abeta and PP2A-C proteins in colorectal cancers. Oncol Rep 11:655–659.
54. Mochida S, Hunt T. 2012. Protein phosphatases and their regulation in the control of mitosis. EMBO Rep 13:197–203. https://doi.org/10.1038/embor.2011.263.
55. Mochida S, Ikeo S, Gannon J, Hunt T. 2009. Regulated activity of PP2A-B55 delta is crucial for controlling entry into and exit from mitosis in *Xenopus* egg extracts. EMBO J 28:2777–2785. https://doi.org/10.1038/emboj.2009.238.
56. Mochida S, Maslen SL, Skehel M, Hunt T. 2010. Greatwall phosphorylates an inhibitor of protein phosphatase 2A that is essential for mitosis. Science 330:1670–1673. https://doi.org/10.1126/science.1195689.
57. Reshi I, Nisa MU, Farooq U, Gillani SQ, Bhat SA, Sarwar Z, Nabi N, Fazili KM, Andrabi S. 2020. AKT regulates mitotic progression of mammalian cells by phosphorylating MASTL leading to PP2A inactivation. Mol Cell Biol 40:e00366-18. https://doi.org/10.1128/mcb.00366-18.
58. Li S, Szymborski A, Miron MJ, Marcellus R, Binda O, Lavoie JN, Branton PE. 2009. The adenovirus E4orf4 protein induces growth arrest and mitotic catastrophe in H1299 human lung carcinoma cells. Oncogene 28:390–400. https://doi.org/10.1038/onc.2008.393.
59. Paradisi A, Creveaux M, Gibert B, Devailly G, Redoulez E, Neves D, Cleyssac E, Treilleux I, Klein C, Niederfellner G, Cassier PA, Bernet A, Mehlen P. 2013. Combining chemotherapeutic agents and netrin-1 in-

terference potentiates cancer cell death. EMBO Mol Med 5:1821–1834. https://doi.org/10.1002/emmm.201302654.
60. Grandin M, Meier M, Delcros JG, Nikodemus D, Reuten R, Patel TR, Goldschneider D, Orriss G, Krahn N, Boussouar A, Abes R, Dean Y, Neves D, Bernet A, Depil S, Schneiders F, Poole K, Dante R, Koch M, Mehlen P, Stetefeld J. 2016. Structural decoding of the netrin-1/UNC5 interaction and its therapeutical implications in cancers. Cancer Cell 29:173–185. https://doi.org/10.1016/j.ccell.2016.01.001.
61. Nolan RD, Lapetina EG. 1990. Thrombin stimulates the production of a novel polyphosphoinositide in human platelets. J Biol Chem 265: 2441–2445.
62. Subramanian A, Tamayo P, Mootha VK, Mukherjee S, Ebert BL, Gillette MA, Paulovich A, Pomeroy SL, Golub TR, Lander ES, Mesirov JP. 2005. Gene set enrichment analysis: a knowledge-based approach for interpreting genome-wide expression profiles. Proc Natl Acad Sci U S A 102:15545–15550. https://doi.org/10.1073/pnas.0506580102.